AD-A127 865 CONTACT-POTENTIAL AND SURFACE-CHARGE EFFECTS IN ATMOSPHERIC-ELECTRICAL INSTRUMENTATION(U) NAVAL RESEARCH LAB WASHINGTON DC J C WILLETT ET AL. 1/1

UNCLASSIFIED 26 APR 83 NRL-MR-5063 F/G 14/2 NL

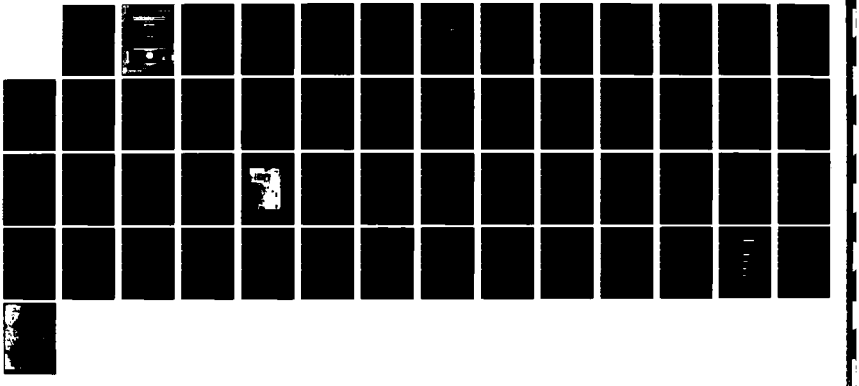

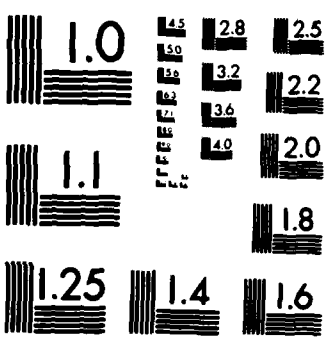

SECURITY CLASSIFICATION OF THIS PAGE (When Data Entered)

REPORT DOCUMENTATION PAGE		READ INSTRUCTIONS BEFORE COMPLETING FORM
1. REPORT NUMBER NRL Memorandum Report 5063	2. GOVT ACCESSION NO.	3. RECIPIENT'S CATALOG NUMBER
4. TITLE (and Subtitle) CONTACT-POTENTIAL AND SURFACE-CHARGE EFFECTS IN ATMOSPHERIC-ELECTRICAL INSTRUMENTATION		5. TYPE OF REPORT & PERIOD COVERED Interim report on a continuing NRL problem. 6. PERFORMING ORG. REPORT NUMBER
7. AUTHOR(s) J. C. Willett and J. C. Bailey		8. CONTRACT OR GRANT NUMBER(s)
9. PERFORMING ORGANIZATION NAME AND ADDRESS Naval Research Laboratory Washington, D.C. 20375		10. PROGRAM ELEMENT, PROJECT, TASK AREA & WORK UNIT NUMBERS 61153N; RR033-02-42; 43-1106-0-3
11. CONTROLLING OFFICE NAME AND ADDRESS		12. REPORT DATE April 26, 1983 13. NUMBER OF PAGES 53
14. MONITORING AGENCY NAME & ADDRESS(if different from Controlling Office)		15. SECURITY CLASS. (of this report) UNCLASSIFIED 15a. DECLASSIFICATION/DOWNGRADING SCHEDULE

16. DISTRIBUTION STATEMENT (of this Report)

Approved for public release; distribution unlimited.

17. DISTRIBUTION STATEMENT (of the abstract entered in Block 20, if different from Report)

18. SUPPLEMENTARY NOTES

This work was supported in part by NASA's Marshall Space Flight Center and Langley Research Center.

19. KEY WORDS (Continue on reverse side if necessary and identify by block number)

Atmospheric electricity	Surface physics
Field mill	Electret
Contact potential	Volta potential

20. ABSTRACT (Continue on reverse side if necessary and identify by block number)

Various investigators have noted deleterious effects on atmospheric electrical measurements due to contact potentials between different metal parts of the apparatus. A less familiar error source of comparable magnitude arises from charge patches which apparently can be deposited on thin insulating films common to the surfaces of many metals. These phenomena seem never to have been studied in the atmosphere, where variable humidity and surface contamination complicate the situation.

(Continues)

DD FORM 1 JAN 73 1473 EDITION OF 1 NOV 65 IS OBSOLETE
S/N 0102-014-6601

SECURITY CLASSIFICATION OF THIS PAGE (When Data Entered)

20. ABSTRACT (Continued)

Two laboratory experiments have been conducted to investigate these error sources with a view toward minimizing their effects by suitable choice of materials. The contact potentials between various metal plates before and after weathering were measured by the nulling potentiometer method in an ionization chamber. The local Volta-potential perturbations due to artificially deposited surface-charge patches were measured on several metal plates by spinning them on a lathe. Of the metals tested, stainless steel and rhodium plate were found to be the best in almost all respects. Surprisingly, gold-plated samples exhibited particularly large variability and sensitivity to weathering.

CONTENTS

CONTACT-POTENTIAL AND SURFACE-CHARGE EFFECTS IN ATMOSPHERIC-ELECTRICAL INSTRUMENTATION

I. INTRODUCTION

There are two electrical considerations involved in the choice of metals to be used in construction of an electric field mill. It is well known that contact potentials between the cover and stator of a conventional shutter mill, or between the rotor and stators of a split-stator mill, can give rise to spurious readings. Although the cylindrical mill design largely eliminates this problem, contact potentials between rotating and stationary parts can still give rise to errors. Less familiar but similar spurious fields can arise from patches of surface charge which may build up on natural dielectric films at the interface between certain metals and the atmosphere. These charge layers cause "potential differences" between the interior and exterior of the metal which resemble changes in the work function of the surface but which vary with the charge density in the layer. For these reasons it is appropriate to investigate the surface properties of possible materials before choosing one for the construction of field mills or other atmospheric-electrical instrumentation.

The contact potential, or Volta-potential difference[1], between two metals was shown by Millikan (1921) to be nearly equal and opposite to the difference between the work functions of their surfaces. Since considerable effort has been devoted to the measurement of work functions, one might think that the necessary data would be available in standard references. Unfortunately, these measurements have almost invariably been made on chemically clean samples in hard vacuum because the work function is known to be very sensitive to surface contamination. We are concerned in field-mill design with surfaces exposed to air and water vapor and having variable surface contamination and oxide layers, so the existing data are nearly irrelevant for our purposes. Although previous designers have undoubtedly

[1]Although the "contact potential" between two metal samples is, strictly speaking, equivalent to the "Volta potential difference" between the two metals *in contact*, these terms will be used interchangeably in this report.

Manuscript approved February 4, 1983.

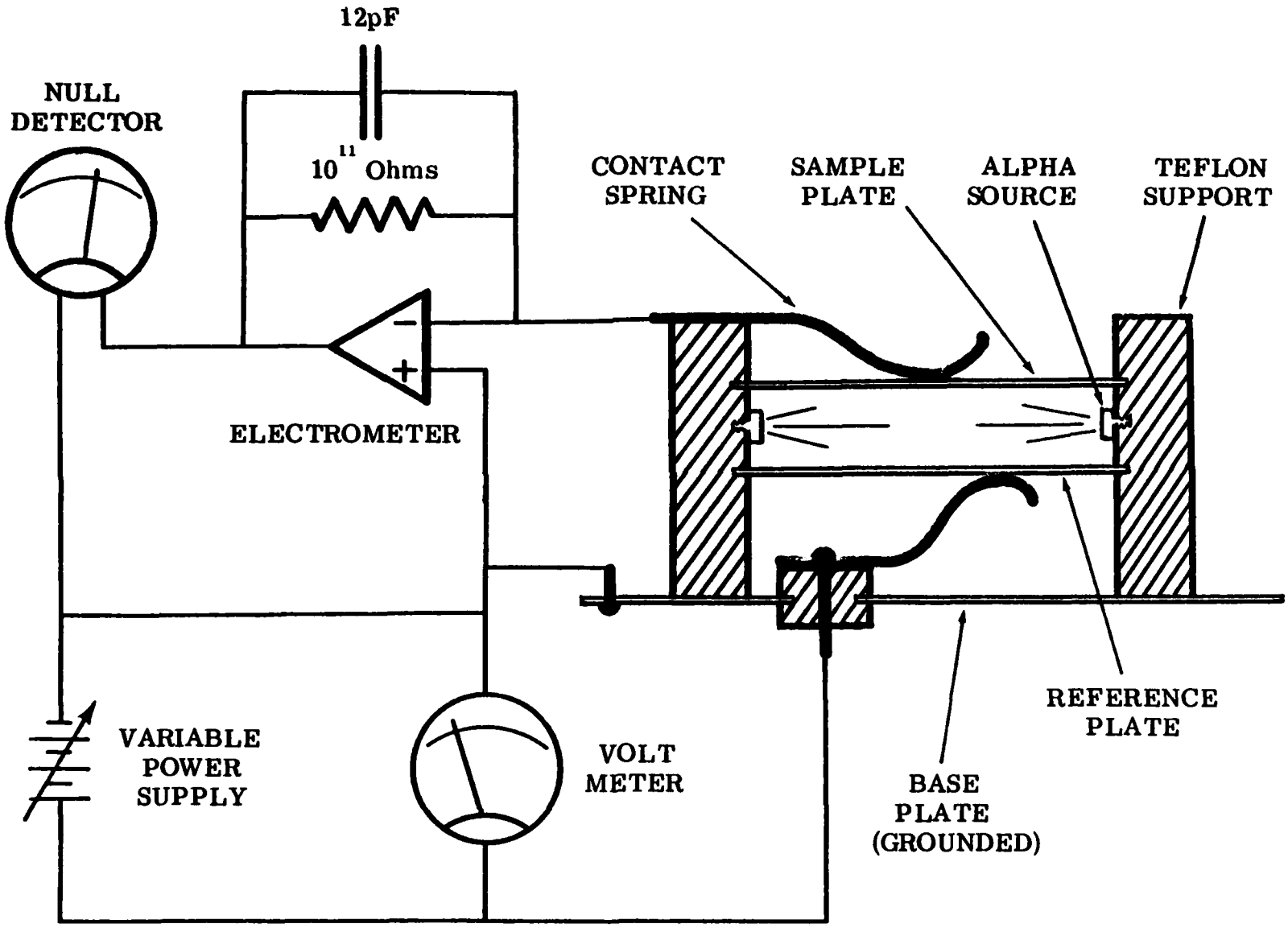

Figure 1 - Conceptual diagram for the ion chamber and circuit diagram for the associated nulling potentiometer. The power supply is adjusted until the voltage applied to the reference plate is sufficient to balance the contact potential between it and the sample plate, as verified by zero ion current flowing in the chamber.

addressed this problem, there appears to be little or no useful information published in the literature. It was therefore decided to make a series of contact-potential measurements on commonly used metals in air.

Two sets of experiments carried out at NRL are described here. In the first set, contact potentials between pairs of metal plates were measured in an ionization chamber with a technique referred to herein as the "nulling potentiometer method". The magnitude and variability of the contact potentials and their sensitivity to the cleanliness and degree of weathering of the surfaces were evaluated by this approach. In the second set of experiments, the variability of the Volta potential with position on the surface of several metal plates was investigated by spinning them on a lathe. This approach, referred to herein as the "capacitive probe method", allowed the contact potentials between different metals and different samples of the same metal to be assessed in another way. More importantly, it enabled us to explore the effects of artificial charge deposition on the electrical properties of various metal surfaces.

II. NULLING POTENTIOMETER METHOD

A pair of flat metal plates to be measured was inserted facing each other into slots in the Teflon (TM)[2] walls of a small enclosure as illustrated in Figure 1. The rectangular parallel-plate capacitor thus formed had a spacing of 1.44 cm and a geometrical area of 95.3 cm^2. This air space was loosely sealed by perpendicular Teflon (TM) walls on all four sides and ionized by six small, electrically isolated, 7.5 μCi, Americium alpha sources mounted on two opposing walls. One plate was connected to a variable power supply whose output voltage was accurately measured, and the other plate was attached with highly insulated, low-capacitance wiring to an electrometer current meter. In operation, the power supply was adjusted until a null was obtained on the current meter, indicating that the electric field vanished between the two plates inside the chamber. Then the Volta-potential difference was read from the power supply's voltmeter.

[2]"Teflon" is a registered trademark of Dupont.

This nulling potentiometer technique of measuring the contact potential has several advantages over other possible approaches. The high ionization inside the chamber not only serves to confine the measurement to the facing sides of the two plates, making the effective capacitance essentially equal to the geometrical, parallel-plate capacitance, but also eliminates charge build-up on the insulators and alpha sources inside the chamber. Furthermore, the presence of air in the chamber does not interfere with the measurement. And last, but not least, the method is quick, easy, and requires no sophisticated equipment.

Proper behavior of the chamber and measuring systems was verified as follows. Based on the geometric chamber capacitance of 5.86 pF, the conductivity between the plates was calculated from the slope of the measured current-voltage characteristic. Both polar conductivities were found to be 1.6×10^{-10} mho/m -- about four orders of magnitude higher than typical values in the lower atmosphere. From the saturation current of 3.0×10^{-9} A flowing in the chamber when the voltage was raised above 200V, the ion-production rate was deduced to be 1.4×10^{14} pairs/m^3-sec -- some eight orders of magnitude larger than the cosmic ray production rate near the earth's surface. If we assume that condensation nuclei are negligible as ion sinks and take a value of 1.6×10^{-12} m^3/sec (Hoppel, 1977) for the small-ion recombination coefficient, this production rate implies polar ion densities of 9.2×10^{12} m^{-3} and ion lifetimes of 68 ms. Assuming a mobility of 1.2×10^{-4} m^2/volt-sec (Mohnen, 1977), which may be somewhat small for ions this young, we estimate the polar conductivities as 1.8×10^{-10} mho/m, in excellent agreement with the measured value. The short ion lifetime implies that the chamber will reach equilibrium very rapidly after new plates are installed. The high conductivity implies a chamber resistance of only 9.4×10^9 ohms -- low enough for an easily measurable current to flow at typical operating voltages.

Basic Chamber Measurements. Since we are primarily interested in aircraft applications, where light weight is an asset, aluminum is an obvious candidate for a field-mill material. We therefore made a number of plates of 2024-alloy aluminum for testing, both uncoated and plated with various other metals. Uncoated plates were prepared in three ways: 1)

TABLE 1. DESIGNATIONS OF SAMPLE PLATES

AU1	Gold Plate	On Ni over Cu plated on 2024-Alloy Al
AU2	" "	" " " " " " " " "
AU3	" "	" " " " " " " " "
RH1	Rhodium Plate	" " " " " " " " "
RH2	" "	" " " " " " " " "
RH3	" "	" " " " " " " " "
CR1	Chromium Plate	" " " " " " " " "
CR2	" "	" " " " " " " " "
CR3	" "	" " " " " " " " "
SS1	304-Alloy Stainless Steel	
SS2	" " " "	
SS3	" " " "	
SS4	" " " "	
AI1	Iridite (TM) Dipped	2024-Alloy Aluminum
AI2	" " "	" " " "
AI3	" " "	" " " "
AB1	Bright-Dipped	" " " "
AB2	" "	" " " "
AB3	" "	" " " "
AW4	Untreated	" " " "
PB1	Bright-Dipped	Pure Aluminum (2S-Alloy)
PB2	" "	" " " " "
PB3	" "	" " " " "
PW4	Untreated	" " " " "

TABLE 2. INITIAL MEASUREMENTS (VOLTS)

Pair	Date (1980) 4/14	4/15	4/17	4/18	4/21	4/22	4/24	4/25	4/28	4/29
AU1, AU2	+.049	+.160	+.179							
AU1, AU3	+.002							(-.027)	(-.171)	
AU1, RH1	-.065	+.036	+.089							
AU1, RH2	-.064									
AU1, RH3	-.068					(+.029)	(+.043)			
AU1, CR2	+.304	+.428	+.490				(+.448)	(+.345)		
AU1, SS1	+.075	[+.122]	[+.167]							
AU1, SS2		+.164	+.260							
AU1, SS3		+.136	+.221							
AU1, SS4		+.130			(+.111)	(+.105)				
AU1, AI1		+.957	+.986	(+.939)						
AU1, AI2		+.937								
AU1, AI3		+.951								
AU1, AB1		+1.054	+1.080						(+.888)	(+.867)
AU1, AW4		+.591	+.628							
AU1, PB1		+1.095	+1.131							
AU1, PW4		+.692	+.692							
AI1, AU1		(-.957)	-.985	-.939						
AI1, AU2				-.792						
AI1, AU3				-.892				(-.933)	(-1.000)	
AI1, RH1			-.875	-.868	[-.850]					
AI1, RH2					-.862					
AI1, RH3					-.870	(-.888)	(-.854)			
AI1, CR2			-.470				(-.472)	(-.520)		
AI1, SS1			-.791	[-.797]						
AI1, SS2				-.728						
AI1, SS3				-.757						
AI1, SS4				-.767	(-.753)	(-.791)				
AI1, AI2			-.002	-.004						

TABLE 2. INITIAL MEASUREMENTS (VOLTS) (continued)

Pair	Date (1980) 4/14	4/15	4/17	4/18	4/21	4/22	4/24	4/25	4/28	4/29
RH3, CR3							+.397			
RH3, SS1						+.158	+.158			
RH3, AI1					(+.870)	+.888	[+.854]			
RH3, AB1						+.977	+.964			
RH3, AW4						+.529				
RH3, PB1						+1.021				
RH3, PW4						+.587				
CR2, AU1	(-.304)						-.448	-.345		
CR2, AU2								-.227		
CR2, AU3								-.357	(-.561)	
CR2, RH1							-.367	-.306		
CR2, CR1							+.070	+.136		
CR2, CR3							-.012	+.052		
CR2, SS1							-.249	-.188		
CR2, AI1			(+.470)				+.472	[+.520]		
AU3, AU1	(-.002)							+.027	+.171	
AU3, AU2								+.135	+.275	
AU3, RH1								+.068	+.185	
AU3, CR1								+.529		
AU3, CR2								+.406	+.561	
AU3, CR3								+.445		
AU3, SS1								+.192	+.296	
AU3, AI1				(+.892)				+.933	[+1.000]	
AU3, AB1									+1.066	
AU3, AB2									+1.102	
AU3, AB3									+1.093	
AB1, AU1		(-1.054)	(-1.080)						-.888	-.867

TABLE 2. INITIAL MEASUREMENTS (VOLTS) (continued)

Pair	Date (1980) 4/14	4/15	4/17	4/18	4/21	4/22	4/24	4/25	4/28	4/29
AI1, AI3			+.012	+.003						
AI1, AB1			+.119		+.090				(+.054)	(+.026)
AI1, AB2					+.125					
AI1, AB3					+.122					
AI1, AW4			-.342							
AI1, PB1			+.146		+.126					
AI1, PB2					+.150					
AI1, PB3					+.154					
AI1, PW4			-.286							
AI2, AI3			+.015							
SS4, AU1		(-.130)			-.111	-.105				
SS4, AU2					+.012					
SS4, AU3					-.121					
SS4, RH1					-.080	-.033				
SS4, CR1						+.367				
SS4, CR2					+.315	+.329				
SS4, CR3						+.314				
SS4, SS1					+.024	+.071				
SS4, SS2					+.053	+.089				
SS4, SS3					+.023	+.060				
SS4, AI1				(+.767)	+.753	+.791				
SS4, AI2						+.782				
SS4, AI3						+.795				
SS4, AB1					+.861	+.897				
SS4, PB1					+.900	+.937				
RH3, AU1	(+.068)					-.029	-.043			
RH3, RH1						+.030	+.027			
RH3, RH2						+.017	+.010			
RH3, CR1							+.476			
RH3, CR2						+.398	+.416			

TABLE 2. INITIAL MEASUREMENTS (VOLTS) (continued)

	Date (1980)									
Pair	4/14	4/15	4/17	4/18	4/21	4/22	4/24	4/25	4/28	4/29
AB1, RH1									-.875	-.838
AB1, CR2									-.489	-.433
AB1, SS1									-.757	-.717
AB1, AI1			(-.119)		(-.090)				-.054	-.026
AB1, AB2									+.052	+.095
AB1, AB3									+.047	+.094

untreated, just as they came from the sheet-metal shop; 2) etched to a satin finish by dipping first in sodium hydroxide and then in nitric acid solutions -- a treatment known as "bright dip"; and 3) Iridite (TM)[3] dipped for a stable, weather-resistant finish produced by a bath of predominantly chromic acid following the bright dip. Other aluminum plates were electroplated with chromium, rhodium, or gold, three metals which can be readily deposited on aluminum (over base coats of copper followed by nickel) to give "corrosion-resistant" surfaces. Plates of pure aluminum (2S-alloy), both untreated and bright dipped, were also measured for comparison with the 2024-alloy. Finally, stainless steel (304-alloy) plates were also tested. The other common structural metals were ignored as either too soft or too susceptible to corrosion without plating or paint.

A total of 25 plates were prepared from the 9 surfaces described above. They will be identified hereafter by the three-character designations listed in Table 1. All of them were washed with soap and water and then wiped with Freon (TM)[4] 113 to bring them to a reasonably clean and reproducible condition. Thereafter, they were handled only by the edges to prevent fingerprints from building up an oil film. All the measurements described below were made in an air-conditioned laboratory at temperatures of 20-25°C and humidities in the 30-60% range. No attempt was made to detect effects of temperature or humidity fluctuations.

The initial procedure involved measuring one plate of nearly every kind against most of the other plates as a check on the consistency and repeatability of the data. In this phase of the experiment 150 measurements were made over a period of 16 days, as listed in Table 2. A measurement is identified by a pair of plates, the first one listed being connected to the power supply and the second to the current meter, and by the date on which the measurement was made. The plates were oriented so that the same side of each was always exposed to the ionized air. The data tabulated are the potentials in volts required on the first plate to produce a null in the current measured to the second plate. Thus, reversing the order of the plates should yield an equal and oposite measurement. That this in fact occurred can be seen in the table.

[3]"Iridite" is a registered trademark of the Richardson Company.
[4]"Freon" is a registered trademark of Dupont.

TABLE 3. RMS DEVIATIONS AMONG SAMPLES (VOLTS)

Surface	Date (1980)	Control	RMS Deviations
AU1,2,3	4/14	AU1	(.021)
RH1,2,3	4/14	AU1	.002
CR1,2,3	4/22	SS4	.022
	4/24	RH3	.034
	4/24	CR2	(.036)
SS2,3,4	4/15	AU1	.015
	4/18	AI1	.017
	4/21	SS4	(.022)
AI1,2,3	4/15	AU1	.088
	4/17	AI1	(.006)
AB1,2,3	4/21	AI1	.016
	4/28	AU3	.015
	4/28	AB1	(.023)
PB1,2,3	4/21	AI1	.012

TABLE 4. MEANS AND RMS DEVIATIONS OF VOLTA POTENTIAL DIFFERENCES VS. RHODIUM (VOLTS)

Second Plate	First Plate: AU1* 4/17	AI1 4/17	SS4 4/21	RH3 4/22	CR2 4/24	AU3 4/25	AB1 4/28	Number of Measurements	Mean Volta Potential Relative to Rhodium	Standard Deviation about Mean	CRC Values Relative to Rhodium
AU1*	-	-.985	-.111	-.029	-.448	+.027	-.888	5	-.027	.045	+.06
RH1	+.089	-.875	-.080	+.030	-.367	+.068	-.875	6	+.023	.018	.00
CR2	+.490	-.470	+.315	+.398	-	X	X	3	+.413	.016	+.14
SS1*	X	X	+.024	+.158	-.249	+.192	-.757	4	+.149	.010	
AI1	+.986	-	+.753	+.888	+.472	+.933	-.054	5	+.876	.018	
AB1	+1.080	+.119	+.861	+.977			-	3	+.988	.017	
AW4	+.628	-.342		+.529				2	+.539	.008	
PB1	+1.131	+.146	+.900	+1.021				3	+1.027	.013	+1.14
PW4	+.692	-.286		+.587				2	+.599	.003	
Number of Measurements	7	7	7	9	4	4	4				
Mean Volta Potential Relative to Rhodium	-.095	+.887	+.112	-	+.410	-.043	+.905				
Standard Deviation about Above Mean	.017	.033	.022	-	.010	.009	.035				

*Aged in the chamber prior to this series of measurements.

Entries in parentheses in Table 2 are not actual observations but rather reflections through zero of measurements made with the plates in reverse order. This has been done to facilitate comparison of data between different days. In the process it was noticed that in some cases a sample appeared to change its characteristics if left in the chamber for an extended period. Therefore, the entry for the first measurement made on each day, which was always a repeat of the last measurement on the previous day, the plates having remained undisturbed in the chamber throughout the intervening period, has been enclosed in a box. Furthermore, vertical bars have been drawn in the table to separate measurements on different days in which one of the plates involved appeared significantly changed by "aging" in the chamber. More will be said about this phenomenon later.

Contact Potential and its Variability. The most obvious question one might ask about the data in Table 2 is whether different samples of the same metal exhibit the same contact potentials. If we include only cases where three similar samples were measured against the same control, or where two of them were measured against the third, on the same day, and if we exclude from this set any cases where one of the three had previously been aged in the chamber, we find 14 cases. These are summarized in Table 3, where the RMS deviations from the mean among the three measured voltages (or among the two measurements and zero in the latter case, these results being given in parentheses) are tabulated.

Another way of assessing the repeatability of these measurements is illustrated in Table 4. Collected there are the cases where a given second plate (down the left side) was measured against a number of first plates (across the top) such that none of the second plates was aged in the chamber during the series. (RH1 and AI1 were not considered aged during the series because they showed no evidence of sensitivity to aging.) Aged first plates have been rigorously excluded, except for AU1 on 4/17. If the assumption is made that the second plates did not change their characteristics during this series of measurements, averages of Volta-potential differences among the first plates can be computed and the fluctuations of individual measurements around these averages can be estimated.

The "Volta-potential" V_A of a metal sample A is defined (see, for example, Adam (1968)) as the electrostatic potential of the space just outside the surface of that sample and is determined to within a constant. Since the power supply on which the nulling potential is measured in our experiments is connected to the first plate, the measurement (A,C) made with first plate A and second plate C actually gives the Volta potential difference V_C-V_A, which has a completely definite value. The Volta-potential difference V_A-V_B between two first plates A and B can then be inferred by differencing the two contact-potential measurements (B,C) - (A,C).

Because of the stability of the rhodium surface suggested by Table 3 and by its resistance to chamber aging (discussed below), RH3 was chosen as the standard against which the contact potential of the other first plates in Table 4 should be measured. For each second plate (row) in the table, the measurement for each first plate in that row has been subtracted from that for RH3, and the means and standard deviations of the resulting Volta-potential differences with respect to rhodium have been tabulated in the last two rows for each column. Finally, these means have been added to each measurement in their respective columns, and the resulting means and standard deviations of the Volta-potential differences of the second plates relative to rhodium have been tabulated in the last two columns but one of Table 4.

From the deviations presented in Tables 3 and 4, it appears that the uncertainty in an individual determination of the contact potential with our apparatus is around 20 mV. The agreement between the two sets of averages in Table 4 is consistent with this estimate except in the cases of AU1 and AB1, whose averages disagree by 68 and 83 mV, respectively. Since the differences among the different metals tested are generally considerably larger than this, our technique is evidently able to yield meaningful data on contact potentials.

Because of the sign conventions involved, the contact potential between samples measured in our experiments should be essentially equal and opposite to the corresponding differences between the work functions of their surfaces. The CRC Handbook (42nd Edition) gives values for the work functions of gold, rhodium, aluminum, and chromium, measured by the contact-

potential method, which can be used to deduce the values of contact potential in the last column of Table 4. Considering that these apply to chemically clean and pure samples in vacuum, the agreement is not bad. In general, we see that active metals, such as bright-dipped pure aluminum, have positive contact potentials relative to noble metals, such as rhodium, of as much as a volt.

The significant difference between the first plates AU1 (after aging) and AU3 (before aging) appearing in the next to last row of Table 4 brings us finally to the question of chamber aging of the samples. In many cases a given first plate was measured on consecutive days (before and after aging) against the same set of second plates. (Recall that a box around an entry in Table 2 indicates that that pair of plates had remained in the chamber since the previous day.) By subtracting the latter measurement of a pair from the former and averaging this difference over all the second plates (except the one which was also aged) in each case, it was possible to measure the effect of aging on each of these first plates. The results of this exercise are presented in Table 5, which shows the average change in the Volta potential (or minus the change in work function) of several plates, and the standard deviation of the individual changes, for pairs of observations ending on the indicated dates.

The results in Table 5 are quite startling. It appears that aging of a plate in the chamber tends to <u>increase</u> its work function by an amount dependent on the metal involved. Even more surprising is the fact that gold appears most affected, followed in descending order of sensitivity by chromium and bright-dipped aluminum. Stainless steel is probably affected slightly, though its average change is approaching the measurement uncertainty, whereas Iridite (TM)-dipped aluminum and rhodium are not significantly altered.

It can be further concluded that this change in work function is persistent. The second aging of AU1 had a smaller affect than the first, and inspection of Table 2 shows that this plate remained more negative than AU2 whenever they are measured against the same first plate. It might be speculated that prolonged exposure to highly ionized air causes chemical reactions to occur on the surfaces of some metals that irreversibly alter their electrical characteristics.

Weathering Tests. So far, the only suggestion that some metals might be more suitable than others for field-mill construction has come from the chamber-aging test. Other measures of the electrical stability of the various surfaces, such as the deviation among different plates of the same material or between the same plate on different days, failed to show large or consisent differences among the samples.

The real question is whether there are major changes in the work functions of metals in the operating environment and whether these changes are reproducible and similar from one sample to another. To address this issue, a program of weathering was carried out. Two of each kind of plate (except AW4 and PW4) were mounted in wooden frames and placed on the roof of the laboratory, exposed to sun, wind, and rain, for periods ranging from eleven days to eight weeks. After exposure, the weathered plates were measured in the chamber for Volta-potential differences relative to AI1. These plates were then washed with warm water, wiped with Freon (TM) 113, and remeasured. As a control against systematic changes in AI1, a number of the plates that remained in pristine condition were also measured in each "weathered" and "washed" run.

This weathering and washing sequence was repeated four times for a total of 14 measurements, the data being presented in Table 6. Since all measurements were relative to AI1 as first plate, only the second plates are listed down the left-hand side, those remaining pristine being identified with an asterisk. Each column of data applies to the run on the date given at the top, alternately weathered for the period shown in parentheses and then washed. The last three rows in the table show the average difference between columns of the measurements for the unweathered plates, their standard deviation from that average, and the number of differences involved, respectively. Since the large difference between AU1 on 7/22 and on 9/22 was judged to be due to a change in that plate alone, it was omitted from the corresponding average. Subsequent to 5/28 a number of plates were dropped from the weathering tests to reduce the measurement burden. In particular, AW4 and PW4 were dropped as being too variable, PB2 and PB3 were omitted as an unlikely structural material, and the gold and rhodium samples were left out because the plating did not hold up well to weathering.

TABLE 5. CHANGE IN VOLTA POTENTIAL DUE TO "CHAMBER AGING" (VOLTS)

First Plate	Date of Second Measurement	Number of Second Plates	Average Change	Standard Deviation
AU1	4/15	3	-.122	.011
AU1	4/17	10	-.044	.030
AI1	4/18	4	-.011	.024
SS4	4/22	8	-.033	.015
RH3	4/24	6	+.003	.012
CR2	4/25	5	-.071	.018
AU3	4/28	5	-.132	.021
AB1	4/29	6	-.041	.012

TABLE 6: VOLTA POTENTIAL RELATIVE TO AI1 IN WEATHERING TESTS (VOLTS)

Second Plate	First Cycle(5/1-5/14) Weathered 5/15	First Cycle(5/1-5/14) Washed 5/16	Second Cycle(5/16-5/27) Weathered 5/27	Second Cycle(5/16-5/27) Washed 5/28	Third Cycle(6/17-7/21) Weathered 7/22	Third Cycle(6/17-7/21) Washed 7/22	Fourth Cycle(7/23-9/16) Weathered 9/22	Fourth Cycle(7/23-9/16) Washed 9/22
AU1*	-.811*	-.850*	-.855*	-.882*	-.805*	-.795*	-.933*	-.928*
AU2	-.931	-.729	-1.070	-.804				
AU3	-.999	-.682	-1.095	-.740				
RH1*	-.802*	-.800*	-.815*	-.824*	-.794*	-.779*	-.795*	-.787*
RH2	-1.020	-.768	-1.024	-.807				
RH3	-.977	-.776	-.992	-.810				
CR1	-.640	-.492	-.692	-.543	-.671	-.553	-.407?	-.505
CR2*	-.376*	-.382*	-.363*	-.375*	-.367*	-.350*	-.326*	-.318*
CR3	-.669	-.507	-.773	-.566	-.687	-.555	-.781	-.512
SS1*	-.674*	-.667*	-.665*	-.671*	-.661*	-.638*	-.636*	-.629*
SS2	-.929	-.680	-.889	-.711	-.897	-.666	-.880	-.590
SS3	-.922	-.673	-.897	-.680	-.896	-.685	-.912	-.615
SS4*	-.689*		-.674*					
AI2	-.252	-.068↓	-.267	-.159	-.411	-.220	-.459	-.221
AI3	-.229	-.193	-.232	-.166	-.384	-.231	-.423	-.238
AB1*	+.068*	+.071*	+.083*	+.068*	+.050*	+.065*	+.077*	+.082*
AB2	-.372	-.055	-.337	-.166	-.548	-.344	-.580	-.334
AB3	-.350	-.061	-.350	-.154	-.588	-.369	-.571	-.241
AW4	-.165	-.182	-.358	-.043				
PB1*	+.121*	+.127*	+.130*	+.114*				
PB2	-.370	+.053	-.290	-.003				
PB3	-.356	+.053	-.287	-.049				
PW4	-.528	-.137	-.383	-.099				

*Unweathered Plate

TABLE 6: VOLTA POTENTIAL RELATIVE TO Al1 IN WEATHERING TESTS (VOLTS) (Continued)

Second Plate	First Cycle(5/1-5/14) Weathered 5/15	First Cycle(5/1-5/14) Washed 5/16	Second Cycle(5/16-5/27) Weathered 5/27	Second Cycle(5/16-5/27) Washed 5/28	Third Cycle(6/17-7/21) Weathered 7/22	Third Cycle(6/17-7/21) Washed 7/22	Fourth Cycle(7/23-9/16) Weathered 9/22	Fourth Cycle(7/23-9/16) Washed 9/22
Average Difference of Unweathered Plates	-.005	+.003	-.014	+.021	+.016	+.006	+.007	
Standard Deviation about Above Average	.018	.012	.008	.036	.004	.017	.001	
Number of Differences	6	6	6	5	5	4	5	

TABLE 7. EFFECT OF WEATHERING
ON THE CONTACT POTENTIAL RELATIVE TO AI1 (VOLTS)

Second Plate	Average Change	Standard Deviation	Number of Weatherings	Standard Deviation Between Samples
AU2 AU3	-.285	.066	4	.062
RH2 RH3	-.213	.030	4	.025
CR1 CR3	-.169	.052	7	.026
SS2 SS3	-.240	.040	8	.020
AI2 AI3	-.139	.073	7	.023
AB2 AB3	-.247	.059	8	.041
AW4	-.149	.235	2	--
PB2 PB3	-.339	.091	4	.027
PW4	-.338	.076	2	--

There are several interesting aspects to this data set that are worthy of comment. First and most obvious is the fact that, in every case but two, a given plate measured more negative relative to AI1 in its weathered state than after subsequent washing. Apparently, the contamination built up during exposure to the elements tends to raise the work function of a metalic surface. Average differences between the weathered and washed condition, along with their standard deviations for the stated number of weathering cycles, have been listed in Table 7 for each kind of exposed plate. The outlier, CR1 on 9/22 (indicated by a question mark in Table 6), has been omitted from these and subsequent statistics. Another badly behaved measurement, AI2 on 5/16 (indicated by the † in Table 6), has also been omitted due to a steady negative drift in its value. Finally, where two plates of the same kind participated in weathering, their data have been counted as separate weathering cycles and combined in the same average.

The last column in Table 7 shows the standard deviation of the differences between samples of the same kind, averaged over all weathered and washed runs. The same numbers of data points apply to these statistics as to the previous averages, although the actual set of measurements used is slightly different due to the two omitted values. Notice that gold has by far the the worst agreement between samples, whereas stainless steel, Iridite (TM)-dipped aluminum, rhodium, bright-dipped pure aluminum, and chromium have the best.

There are two other important questions which can be addressed with the data in Table 6. First, is there evidence of the buildup of an oxide layer or of other permanent modification to the surface of the samples due to weathering? To answer this question, we have plotted in Figure 2 the potentials measured for the various plates after washing (to remove soluble surface films) versus the number of weathering cycles, using the last value before any weathering as the first point. Although CR1 and CR3 were not measured against AI1 before weathering, pre-weathering values were deduced from measurements of these three plates againt CR2 on 4/25.

A straight line has been fitted by least squares to the data plotted in Figure 2 for each kind of plate, and the slopes of these lines (potential vs. weathering cycle number, taking no account of the length of the weathering periods) are listed in Table 8 along with the corresponding

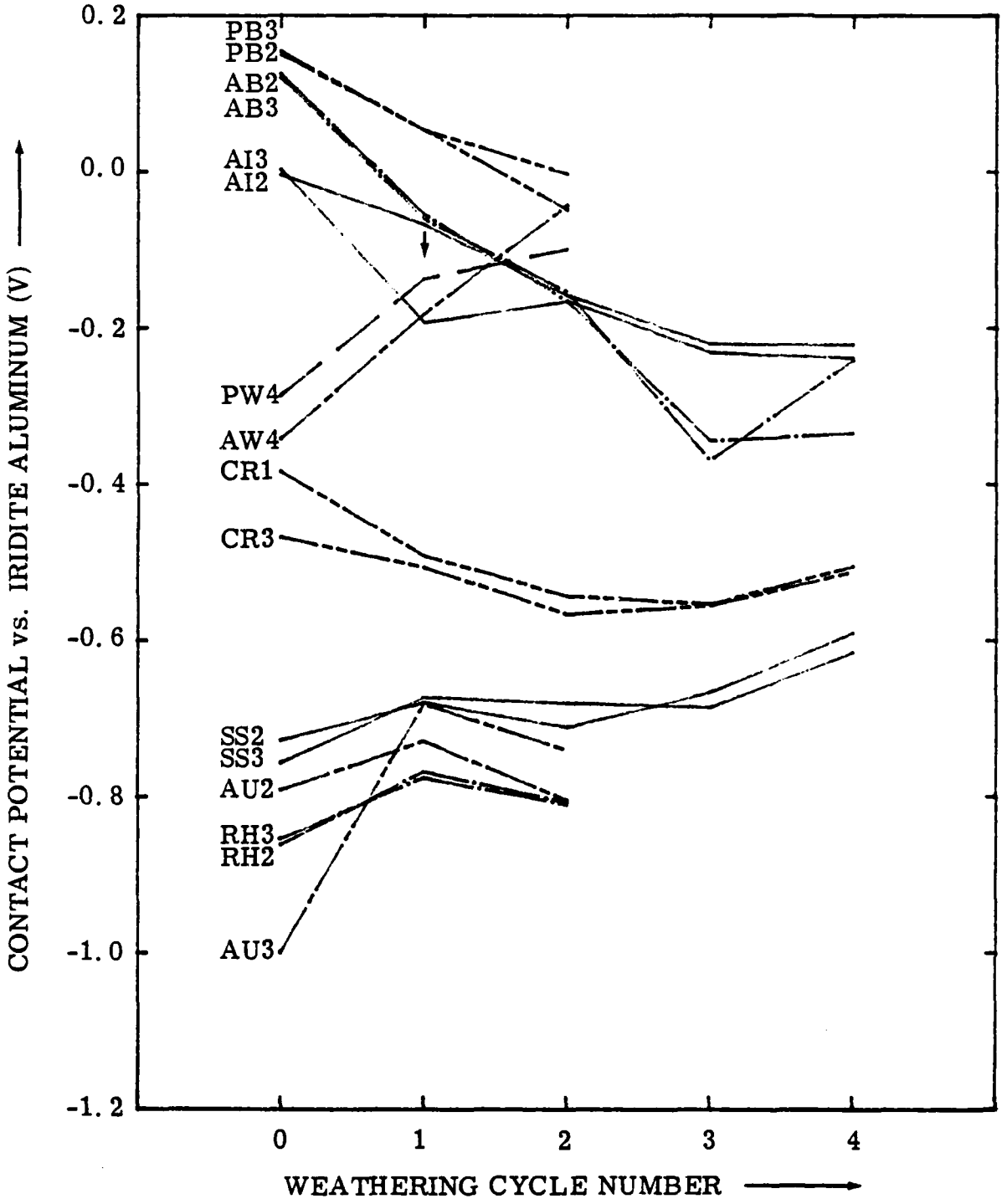

Figure 2 - Nulling potentiometer measurements of contact potential between weathered sample plates of various materials and a control plate of Iridite (TM) aluminum. These measurements were made after washing the sample plates with water and Freon (TM) 113, following the weathering exposure number indicated on the horizontal axis. The data plotted for weathering cycle zero correspond to the last measurements made before the first weathering exposure.

TREND IN WEATHERED SURFACE BEFORE WASHING

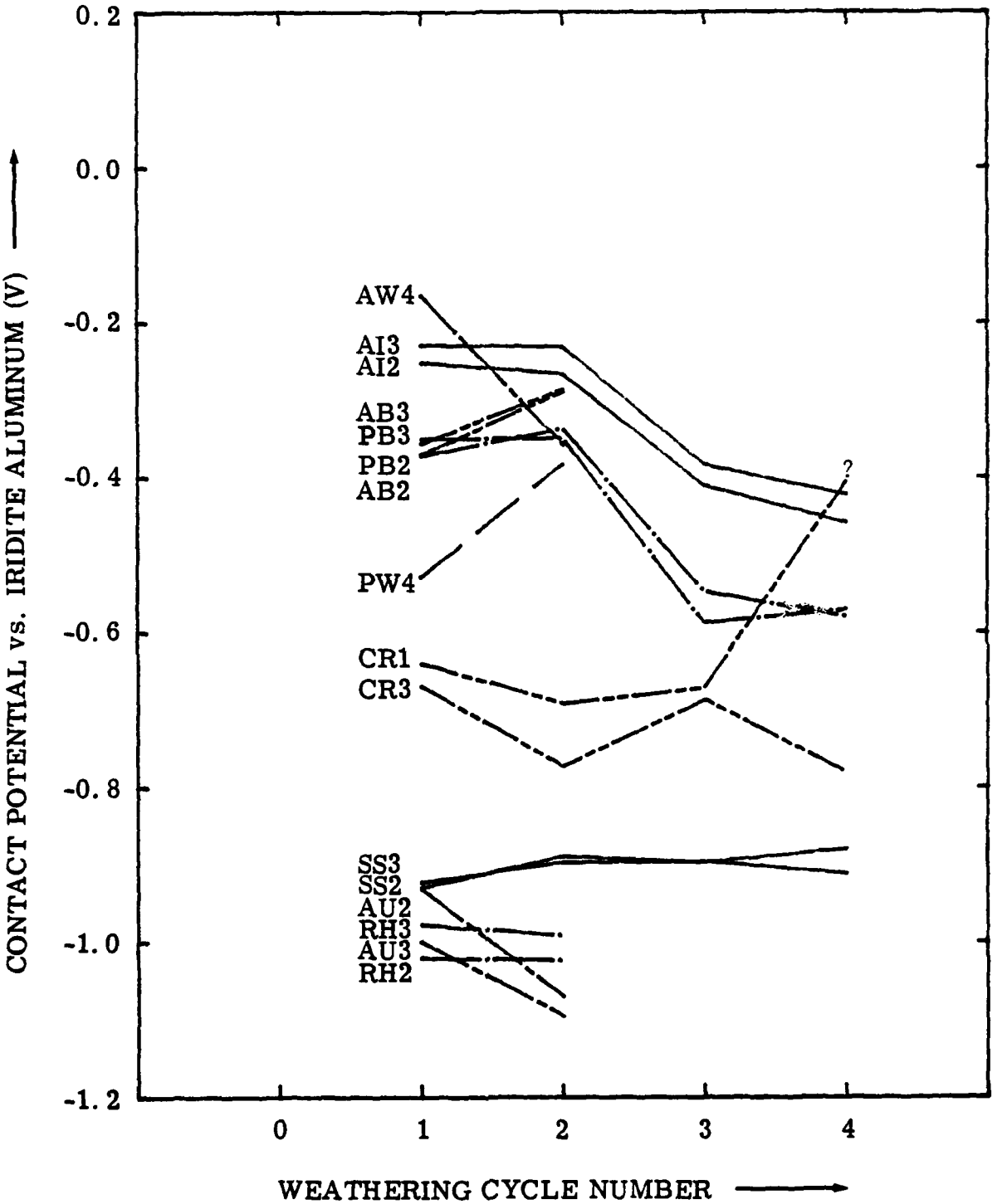

Figure 3 - Same as Figure 2, except that these measurements were made immediately after the indicated weathering exposure, before washing.

TABLE 8. CHANGE IN PLATES AS A FUNCTION OF WEATHERING CYCLE NUMBER (VOLTS)

Second Plate	After Weathering and Washing			Immediately After Weathering		
	Slope of Curve	Correlation Coefficient	Number of Data	Slope of Curve	Correlation Coefficient	Number of Data
AU2 AU3	+.062	+.497	6	-.118	-.917	4
RH2 RH3	+.025	+.571	6	-.010	-.243	4
CR1 CR3	-.022	-.608	10	-.028	-.575	7
SS2 SS3	+.028	+.852	10	+.009	+.607	8
AI2 AI3	-.054	-.874	9	-.082	-.906	8
AB2 AB3	-.112	-.923	10	-.087	-.877	8
AW4	+.150	+.9992	3	-.193	-	2
PB2 PB3	-.089	-.982	6	+.075	-.991	4
PW4	+.094	+.946	3	+.145	-	2

Significance Level of Correlation Coefficient	Number of Data Points							
	3	4	5	6	7	8	9	10
5%	.997	.950	.878	.811	.754	.707	.666	.632
1%	1.000	.990	.959	.917	.874	.834	.798	.765

correlation coefficients for the stated numbers of points. For convenience, the bottom of the table shows the correlation coefficient required for a line fitted to a given number of data points to have a slope significantly different from zero, taken from Fischer (1958). Based on this information, the slopes significant at the 1% level are enclosed in boxes.

From Figure 2 and the associated table it can be seen that several of the surfaces tested show definite evidence of chemical changes. In order of decreasing sensitivity, untreated aluminum, bright-dipped aluminum, bright-dipped pure aluminum, and Iridite (TM)-dipped aluminum have slopes substantially different from zero. Chromium, rhodium, and stainless steel exhibit very small slopes, by contrast, although the last is significantly different from zero.

Perhaps the most important question for field-mill construction is how much the work function of a metal surface is likely to change in the operating environment. This issue can be examined by plotting the measured potentials of the samples in weathered condition (before washing) against weathering cycle number as in Figure 3. The corresponding slopes of fitted lines are again presented in Table 8. In this case, stainless steel far surpasses the others, having a negligible slope and nearly identical potentials on the two samples. Rhodium also looks good; but bright-dipped aluminum, Iridite (TM)-dipped aluminum, and bright-dipped pure aluminum have considerable, statistically significant slopes; and the others show substantial changes from cycle to cycle. This result and the previous one suggest that the Iridite (TM) surface, which looked so good in earlier tests, may not be useful for field mills.

III. CAPACITIVE PROBE METHOD

As mentioned in the introduction, we also wanted to investigate the extent to which charge artificially deposited on the surface of a metal in

air affects its apparent work function[5] In the operating environment such charge deposition might be caused by corona discharge in high fields or by triboelectric charging through impact of dust particles on aircraft instrumentation. Charge can be applied to a spot on a metal surface with corona. To facilitate measurement of the resulting patch of surface charge and to permit the mapping of relative Volta potential over a surface, a new technique has been developed.

A metal sample is mounted on the face plate of a lathe and faced flat. Platings and other surface treatments are then applied as desired. A capacitive probe mounted in the tool holder of the lathe can be brought in close proximity to the flat surface. When the sample is rotated, variations in Volta potential around the circular path traced by the probe induce fluctuations in the surface charge density on the probe, which are measured by a charge amplifier. The output is fed to an oscilloscope triggered by a magnetic pickup so that its sweep is synchronous with the lathe rotation. With proper calibration, the scope then shows a graph of relative Volta potential versus angular position of the sample. The apparatus, shown in Figure 4, is actually a kind of field mill, where the capacitive probe acts as the stator and the rotating sample as the shutter.

A schematic diagram of the electronics for this setup is shown in Figure 5. For rotation periods much shorter than the integration time constant of one second, the charge induced on the probe is transferred to the storage capacitor. Thus a Volta-potential fluctuation ΔV_v from point to point on the sample surface produces an output signal $\Delta V_o = \Delta V_v G C_p / C_s$, where C_s is the storage capacitance, C_p is the capacitance between probe and sample, and -G is the voltage gain of the amplifier stage.

The lathe and sample plate must always remain at ground potential, so calibration can be achieved only by isolating the scope and charge amplifier from ground and applying a test signal to them. This is accomplished by

[5]The term "appararent work function" is used here to denote the "potential difference" between the interior and exterior of a metal, as influenced by artificially deposited surface charge on any dielectric layer as well as by the "intrinsic" work function of the surface. We cannot, of course, measure the apparent work function directly, but only its variability from place to place on a surface or its difference between different surfaces. We will refer to the negative of such differences as "apparent contact potentials" of Volta-potential differences.

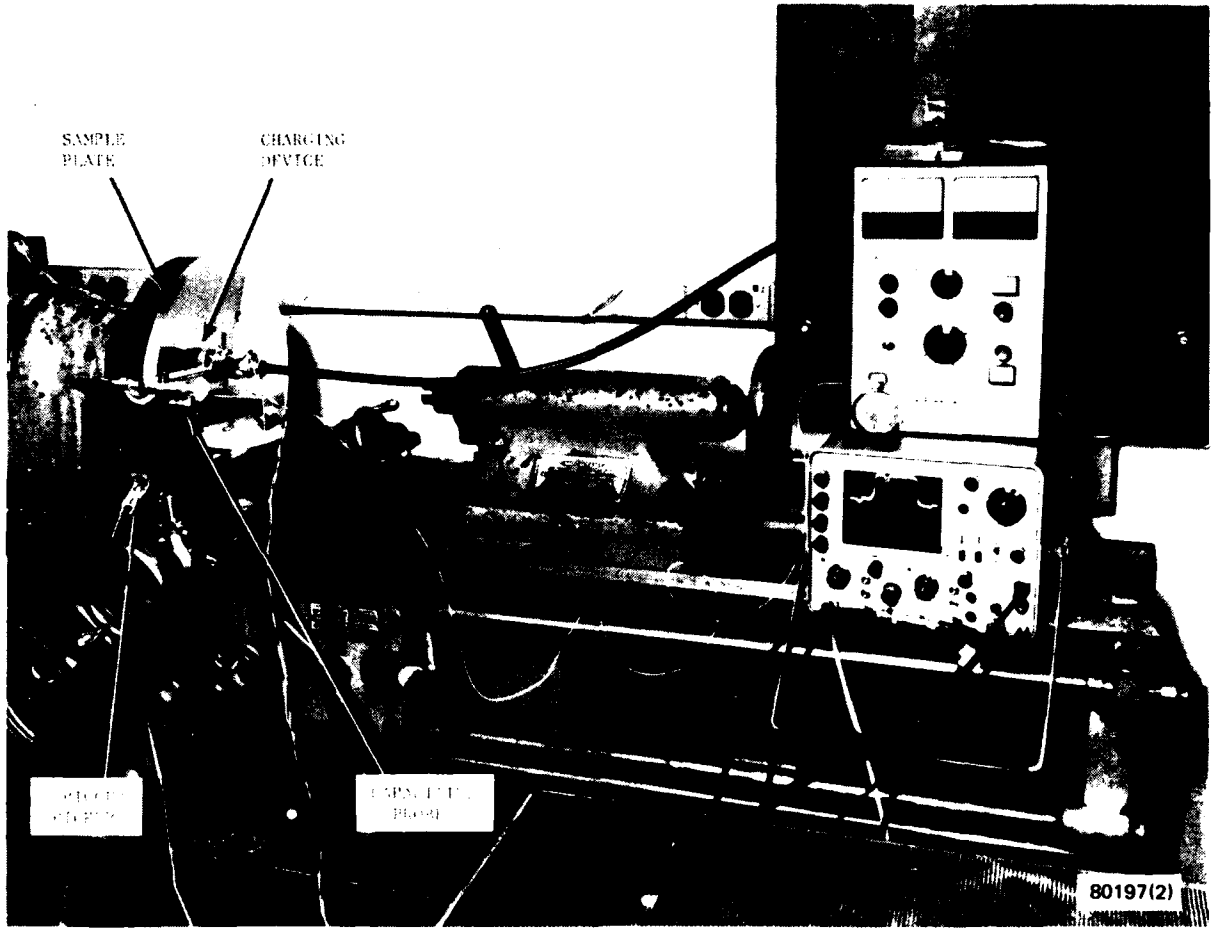

Figure 4 - Experimental apparatus for the capacitive-probe experiment, showing sample plate #1 mounted on the lathe. During a measurement, the oscillscope is triggered by a magnetic pickup and displays the relative Volta potential as a function of angular position along a circular path on the sample plate as it is rotated beneath the probe. In this case the amplitude of the square wave represents the contact potential between Iridite (TM) and bright aluminum, and the large spike represents the perturbation caused by a patch of negative surface charge deposited on the bright surface with the shielded corona-charging device.

placing the switch in the "Cal" position. The test signal is then fed from an oscillator to the charge amplifier, where it induces charge on the probe in the same way that actual Volta-potential fluctuations would. The amplitude of the resulting output can be compared with the test signal on the scope, and the system sensitivity can be adjusted by changing the probe-sample spacing, hence C_p.

Three distinct sample plates were used in this series of experiments. Plate 1, visible in Figure 4, was made of 2024-alloy aluminum, bright-dipped in its entirety and then treated with Iridite (TM) over half of its face. Plate 2 was 304-alloy stainless steel with chromium plate on a 90° sector and rhodium plate on a 180° sector. Plate 3 was 2024-alloy aluminum divided into three 120° sectors of Iridite (TM), chromium plate, and rhodium plate. Although distinct from the samples used in the ion chamber, the various sectors will be referred to by designations introduced in Table 1 above.

Contact Potential and its Variability. The three sample plates provide direct measurements of seven different contact potentials, as listed in Table 9. An example of one such measurement is illustrated in Figure 4, where the square wave (but not the spike) on the scope display represents the contact potential between AI1 and AB1. By assuming AI1 and AI3 to have identical surface properties (as well as RH2 and RH3), we have referred all of these contact potentials to rhodium and ranked the surfaces in ascending order at the bottom of the table.

The first thing to notice about the data in Table 9 is that individual determinations of contact potential by the capacitive probe method exhibit about twice the uncertainty of those by the nulling potentiometer method. This may be due in part to calibration and measurement uncertainties, but it is also due to the intrinsic variabilities of the surfaces involved. To investigate the latter aspect, we recorded the peak-to-peak amplitude of the fluctuations in Volta potential on each surface in Table 10. This was done by measuring the deviations of the scope trace from a horizontal line during the time that the probe remained over a single sector of a sample plate (refer to Figure 4). Not only do some metals show considerably lower variability than others (as ranked in the last row of the table), but also

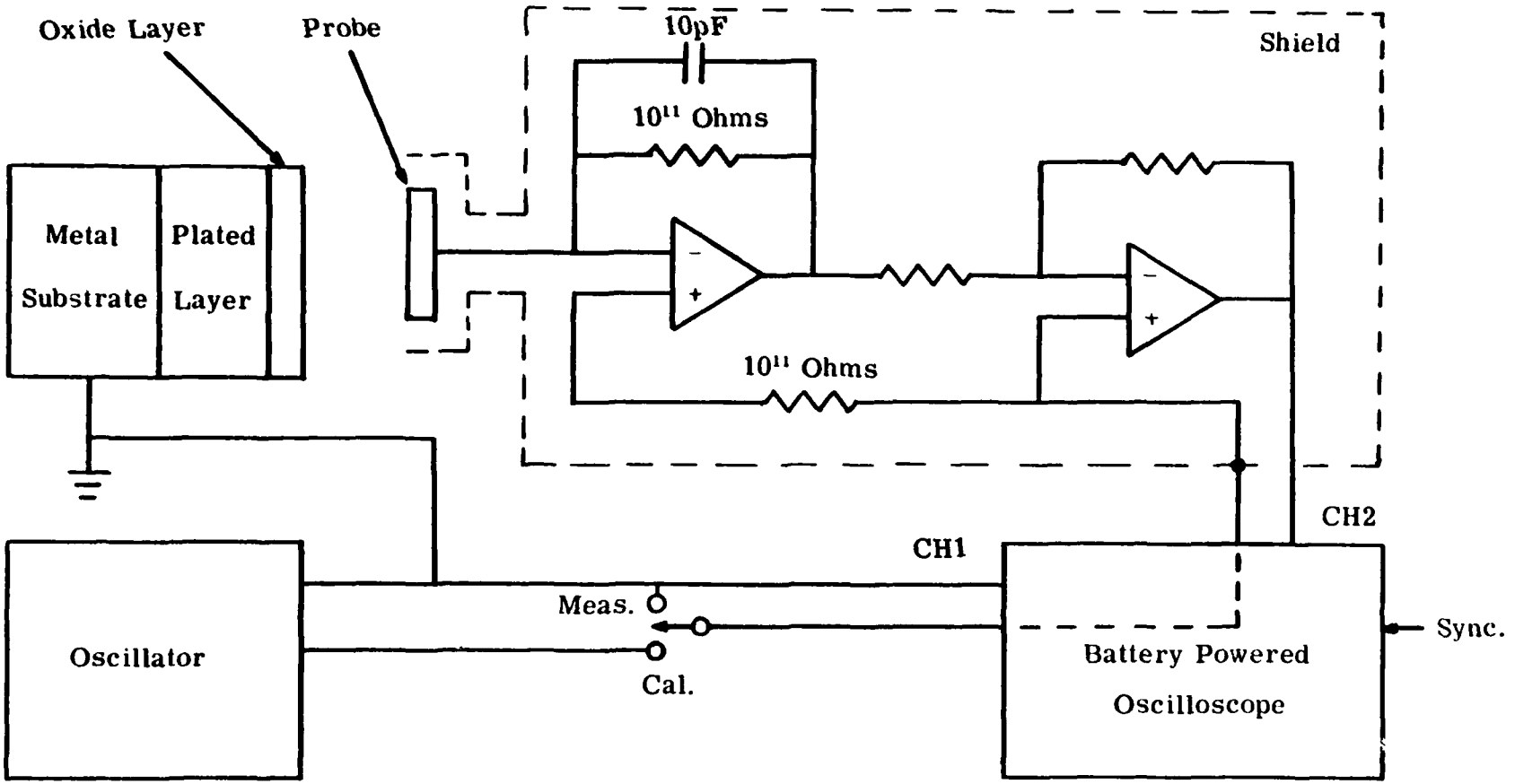

Figure 5 - Circuit diagram for the capacitive probe and charge amplifier. With the switch in the "Calibrate" position a square wave of known amplitude is applied to the floating common point of the charge amplifier, resulting in an apparent Volta-potential signal between the probe and the sample plate.

Table 9. Daily Contact Potentials (Volts)

Date	CR2 −SS2	SS2 −RH2	CR2 −RH2	Date	CR3 −AI3	AI3 −RH3	CR3 −RH3	Date	AB1 −AI1
3/2/82	.350	.316	.656	4/1/82	.521	.165	.698	5/20/82	.605
3/3/82	.310	.245	.575	4/2/82	.642	.110	.750	5/21/82	.660
3/4/82	.340	.221	.579	4/5/82	.660	.100	.760	5/24/82	.762
3/9/82	.358	.283	.642	4/7/82	.660	.100	.760	5/25/82	.744
3/10/82	.338	.208	.544	4/8/82	.620	.155	.770	5/26/82	.718
3/11/82	.347	.209	.542	4/9/82	.615	.118	.730	5/28/82	.804
3/15/82	.398	.288	.682	4/12/82	.620	.140	.760	6/1/82	.784
3/16/82	.396	.211	.600	4/14/82	.640	.120	.780	6/2/82	.680
3/17/82	.358	.189	.560	4/15/82	.625	.123	.758	6/4/82	.840
3/18/82	.363	.140	.525	4/16/82	.616	.141	.763	6/8/82	.802
3/19/82	.350	.178	.508	4/26/82	.610	.142	.760	6/9/82	.800
3/25/82	.364	.209	.580	4/27/82	.490	.213	.700	6/10/82	.800
3/26/82	.382	.161	.523	4/28/82	.524	.181	.702	6/11/82	.760
3/29/82	.375	.199	.580	4/30/82	.700	.158	.762	6/15/82	.764
3/31/82	.340	.138	.496	5/3/82	.610	.098	.714	6/18/82	.800
-	-	-	-	5/5/82	.624	.101	.736	-	-
-	-	-	-	5/17/82	.620	.119	.736	-	-
-	-	-	-	5/19/82	.621	.097	.710	-	-
MEAN	.358	.213	.573		.612	.132	.742		.755
σ	.023	.052	.054		.052	.032	.027		.064
N	15	15	15		18	18	18		15

	AI3	SS2	CR2	CR3	AB1
Volta Potential Relative to Rhodium	.132	.213	.573	.742	.887
Order Relative to Rhodium	1	2	3	4	5

Table 10. Intrinsic Variation in Volta Potential Over A Sector (Volts)

Date	CR2	SS2	RH2	Date	CR3	AI3	RH3	Date	AB1	AI1
3/2/82	.070	.040	.080	4/1/82	.027	.028	.044	5/20/82	.080	.145
3/4/82	.020	.022	.020	4/2/82	.030	.024	.040	5/21/82	.040	.071
3/9/82	.020	.006	.053	4/5/82	.024	.027	.040	5/24/82	.020	.072
3/10/82	.021	.019	.036	4/7/82	.021	.052	.037	5/25/82	.030	.072
3/11/82	.043	.008	.021	4/8/82	.021	.034	.028	5/26/82	.040	.071
3/15/82	.019	.041	.019	4/9/82	.027	.024	.028	5/28/82	.043	.074
3/16/82	.011	.010	.056	4/12/82	.024	.024	.033	6/1/82	.030	.075
3/17/82	.018	.022	.026	4/14/82	.019	.026	.041	6/2/82	.040	.054
3/18/82	.027	.022	.019	4/15/82	.021	.024	.024	6/4/82	.020	.052
3/19/82	.039	.019	.028	4/16/82	.020	.028	.028	6/8/82	.040	.071
3/25/82	.015	.013	.045	4/26/82	.021	.032	.035	6/9/82	.041	.070
3/26/82	.019	.010	.028	4/27/82	.020	.036	.032	6/10/82	.041	.062
3/29/82	.015	.012	.046	4/28/82	.049	.028	.055	6/11/82	.032	.060
3/31/82	.010	.008	.021	4/30/82	.021	.025	.036	6/15/82	.018	.071
-	-	-	-	5/3/82	.029	.043	.028	6/18/82	.057	.071
-	-	-	-	5/5/82	.030	.036	.029	-	-	-
-	-	-	-	5/17/82	.045	.032	.032	-	-	-
-	-	-	-	5/19/82	.030	.032	.028	-	-	-
MEAN	.025	.018	.036		.027	.031	.034		.038	.073
σ	.016	.011	.018		.008	.008	.008		.016	.021
N	14	14	14		18	18	18		15	15
ORDER	2	1	6		3	4	5		7	8

Table 11. Daily Contact Potential After Washing (Volts)

Date	CR2 −SS2	SS2 −RH2	CR2 −RH2	Date	CR3 −AI3	AI3 −RH3	CR3 −RH3	Date	AB1 −AI1
3/2/82	.316	.210	.508	4/1/82	.238	.386	.620	5/20/82	.480
3/3/82	.335	.178	.520	4/2/82	.256	.402	.660	5/21/82	.480
3/4/82	.310	.159	.461	4/5/82	.200	.445	.662	5/24/82	.498
3/9/82	.319	.200	.503	4/7/82	-.060	.678	.650	5/25/82	.501
3/10/82	.323	.181	.501	4/8/82	.120	.520	.643	5/26/82	.441
3/11/82	.320	.200	.493	4/9/82	.283	.400	.684	5/28/82	.520
3/15/82	.390	.255	.660	4/12/82	.395	.342	.740	6/1/82	.460
3/16/82	.389	.161	.558	4/14/82	.362	.365	.739	6/2/82	.380
3/17/82	.341	.182	.516	4/15/82	.256	.443	.717	6/4/82	.540
3/18/82	.380	.155	.532	4/16/82	.330	.394	.715	6/8/82	.382
3/19/82	.339	.141	.500	4/26/82	.152	.543	.696	6/9/82	.546
3/25/82	.366	.197	.558	4/27/82	.220	.459	.678	6/10/82	.559
3/26/82	.358	.161	.504	4/28/82	.280	.423	.708	6/11/82	.422
3/29/82	.354	.162	.520	4/30/82	.398	.357	.759	6/15/82	.617
3/31/82	.358	.156	.500	5/3/82	.343	.352	.702	6/18/82	.542
-	-	-	-	5/5/82	.356	.408	.760	-	-
-	-	-	-	5/17/82	.250	.438	.700	-	-
-	-	-	-	5/19/82	.300	.399	.702	-	-
Group Average	.346	.180	.522		.260	.431	.696		.491
σ	.027	.029	.045		.111	.082	.040		.067
N	15	15	15		18	18	18		15

	AI3	SS2	CR2	CR3	AB1
Volta Potential Relative to Rhodium	.431	.180	.522	.696	.922
Order Relative to Rhodium	2	1	3	4	5

Table 12. Intrinsic Variation in Volta Potential Over a Sector After Washing (Volts)

Date	CR2	SS2	RH2	Date	CR3	AI3	RH3	Date	AB1	AI1
3/4/82	.009	.008	.018	4/1/82	.020	.032	.028	5/20/82	.032	.040
3/9/82	.011	.008	.016	4/2/82	.019	.022	.025	5/21/82	.013	.013
3/10/82	.015	.008	.020	4/5/82	.012	.020	.026	5/24/82	.018	.018
3/11/82	.009	.003	.021	4/7/82	.032	.032	.032	5/25/82	.030	.076
3/15/82	.010	.006	.052	4/8/82	.020	.021	.024	5/26/82	.052	.016
3/16/82	.002	.008	.026	4/9/82	.020	.020	.020	5/28/82	.024	.031
3/17/82	.010	.004	.009	4/12/82	.020	.028	.024	6/1/82	.012	.045
3/18/82	.014	.020	.014	4/14/82	.015	.032	.022	6/2/82	.035	.025
3/19/82	.016	.010	.012	4/15/82	.008	.020	.020	6/4/82	.016	.020
3/25/82	.010	.020	.023	4/16/82	.012	.026	.020	6/8/82	.021	.020
3/26/82	.016	.008	.018	4/26/82	.012	.021	.022	6/9/82	.012	.024
3/29/82	.008	.004	.012	4/27/82	.023	.019	.024	6/10/82	.030	.070
3/31/82	.010	.004	.016	4/28/82	.020	.036	.024	6/11/82	.046	.031
-	-	-	-	4/30/82	.020	.041	.032	6/15/82	.041	.111
-	-	-	-	5/3/82	.005	.022	.023	6/18/82	.021	.079
-	-	-	-	5/5/82	.012	.012	.022	-	-	-
-	-	-	-	5/17/82	.025	.012	.024	-	-	-
-	-	-	-	5/19/82	.021	.027	.026	-	-	-
MEAN	.011	.009	.020		.018	.025	.024		.027	.041
σ	.004	.006	.011		.006	.008	.004		.013	.027
N	13	13	13		18	18	18		15	15
ORDER	2	1	4		3	6	5		7	8

the variability of some (particularly those on plate 3) is more stable than that of others.

We had intended to do all of the lathe experiments using "clean" surfaces, since weathering tests had already been performed with the ion chamber. In the course of these measurements, however, it was observed that, although wiping the sample plates with Freon (TM) 113 had little or no effect on their electrical properties, washing with water caused considerable changes. In most cases the contact potential between two sectors was smaller immediately after washing. It gradually returned to its pre-washing level with a time constant on the order of an hour. Immediately after each of the measurements tabulated in Tables 9 and 10, the sample plate was wiped with Freon (TM), washed with water, and remeasured. The results for contact potential and variability after washing are presented in Tables 11 and 12, respectively. Notice that the positions of AI3 and SS2 in the contact-potential order relative to rhodium are reversed by washing and that the variability of every surface is reduced.

The means and standard deviations of the change in contact potential due to washing have been computed over all the washing cycles tabulated in Tables 9 and 11 and are presented in Table 13. Although it is not possible to ascribe a definite fraction of a given change or uncertainty to a particular surface sector, some qualitative conclusions can be drawn. Note that the values are fairly small for the measurements on plate 2, suggesting that the rhodium, stainless steel, and chromium surfaces are fairly insensitive to washing. This inference is substantiated by the CR3-RH3 data from the plate 3, implying that the Iridite (TM) surface is responsible for the large values of change and uncertainty in the CR3-AI3 and AI3-RH3 measurements. No conclusion can be drawn regarding the behavior of bright aluminum, since it was only measured relative to Iridite (TM).

Finally, it is of interest to compare the lathe measurements of contact potential with those described earlier from the ion-chamber experiments. This is done in Table 14, where it can be seen that there is a fair correspondence for stainless steel, chromium, and bright aluminum, but not for Iridite (TM). The agreement is better after washing then before. We have no explanation for the differences between the two measurement techniques other than the suggestion that the high ion density in the chamber may play a role.

Table 13. Changes in Contact Potential Due to Washing (Volts)

	CR2 -SS2	SS2 -RH2	CR2 -RH2	CR3 -AI3	AI3 -RH3	CR3 -RH3	AB1 -AI1
Mean	-.011	-.033	-.051	-.352	+.299	-.045	-.264
σ	.020	.036	.048	.121	.089	.042	.075
N	15	15	15	18	18	18	15

Table 14. Comparison of Contact Potentials Relative to Rhodium Between the Capacitive Probe and Nulling Potentiometer Methods

Surface	Before Washing	After Washing	Ion Chamber
AI1	.132	.431	.887
SS2	.213	.180	.112
CR2	.573	.522	.410
CR3	.742	.696	
AB1	.887	.922	.905

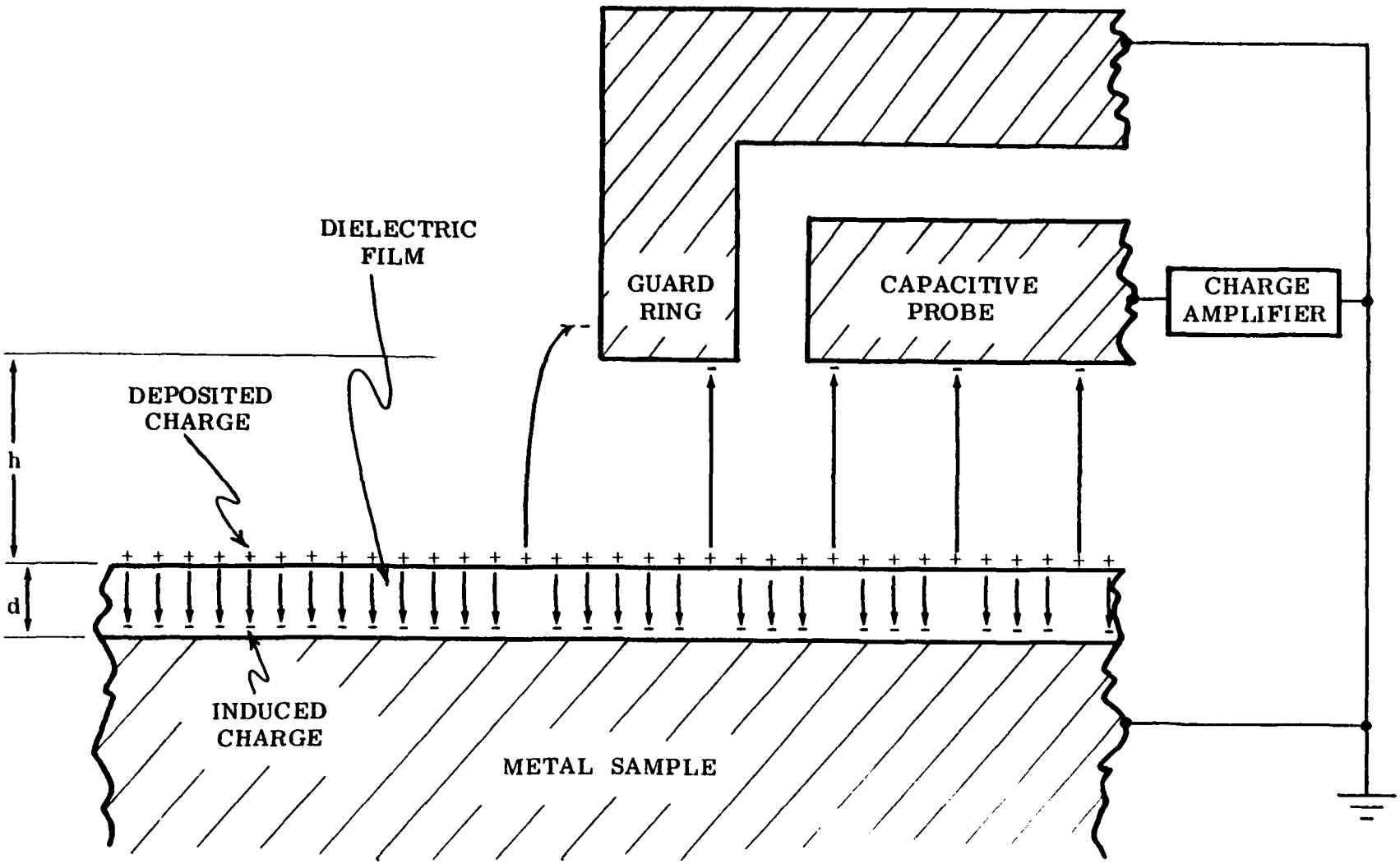

Figure 6 - Conceptual diagram of a charged dielectric layer on a metal substrate, showing its interaction with the capacitive probe. A grounded guard ring shields the probe from external fields and helps to preserve one-dimensional symmetry.

Surface Charging. The primary goal of the lathe experiments was to assess the "chargeability" of various metal surfaces. A simple physical model may help to clarify the situation. With reference to Figure 6, suppose that a thin, uniform dielectric layer of permittivity ε exists on the surface of the metal sample plate. Suppose further that a uniform, net surface-charge density σ is deposited on the outer surface of this insulating layer. The thinness of the dielectric leads to one-dimensional symmetry, with the results that an equal and opposite charge density is induced on the metal-dielectric interface and that all the electric field is confined within the insulating layer. Immediate consequences are that air conductivity is irrelevant and that the charge will decay with a relaxation time determined only by the properties of the dielectric. The potential drop across the layer will be $V_d = \sigma d/\varepsilon$, where d is its thickness.

Now suppose that a flat capacitive probe, grounded to the face plate, is brought close enough to the surface that one-dimensional symmetry prevails. Some of the field lines from the deposited charge will reconnect from the plate to the probe, inducing a charge on it which is measured by our electronics. It is easy to show that, for a probe-to-surface spacing $h \gg d$, this induced charge is given by $q \simeq \varepsilon_0 A V_d/h = V_d C_p$, where ε_0 is the permittivity of air and A is the effective area of the probe. Thus, the apparent work function V_d produced by a surface-charge layer of this sort is indistinguishable (by external measurements with $h \gg d$) from the intrinsic work function of the surface. Surface-charge patches can change measured Volta-potential differences.

Some sort of ionizing device is required to deposit net charge efficiently on a metalic surface. Three different arrangements were tried, as illustrated schematically in Figure 7. The first was a simple corona point brought within about a centimeter of the sample plate and raised to a high potential. This technique was indeed found to produce local perturbations in Volta potential on the exposed surfaces. Some bizarre phenomena were also observed, however, and we were unable to get consistent and repeatable results, so direct corona charging was abandoned.

The second apparatus tried was a radioactive ionizer with a field

applied to cause ions of one sign to drift to the sample plate. It was hoped that this method, which eliminates exposure of the plate to direct corona and its associated high fields, bipolar ionization, and possible chemical changes, would yield more consistent results. Although it was possible to produce weak perturbations of either sign in the Volta potential on certain surfaces by using the appropriate polarity of applied voltage, the degree of charging obtained in this way was small.

The most satisfactory arrangement tried was a shielded corona discharge (to produce a large charge density) in conjunction with an applied field of the same polarity to make the ions drift to the sample plate. This apparatus produced unipolar ion currents of known intensity, as shown in Figure 8, when the corona voltage was held at ±6500V, the point-to-screen gap was 0.97 cm, and the current was measured to a conducting plane 0.76 cm from the screen. This current was nearly an order of magnitude larger than that obtainable from the radioactive ionizer. The shielded source produced repeatable local perturbations in Volta potential, such as the large negative spike on surface AB1 visible in the scope trace of Figure 4. We were convinced that these perturbations were the result of deposited surface-charge patches by their correspondence in sign and magnitude with the polarity and intensity of the applied ion currents. Therefore, the shielded corona apparatus was used in all subsequent charging experiments.

Several general observations should be made about the Volta-potential perturbations produced in this manner. First, they decay gradually with time constants on the order of twenty minutes to an hour, the exact rate depending somewhat on the type of surface and the polarity of charging. Second, the decay rates are not materially affected by increasing the conductivity of the overlying air with radioactive ionization, in agreement with the simple theory expounded above. Third, surface-charge patches can be made to vanish temporarily by washing the sample plate with water (but not with Freon (TM)), but the perturbations gradually reappear over a period of an hour or so.

Although we cannot explain these phenomena in detail, they seem to be generally consistent with the theory of electrets (see, for example Sessler, 1980). According to current work on the subject, the decay times should depend on the concentration, polarity, and mobility of charge carriers in

UNSHIELDED CORONA SOURCE

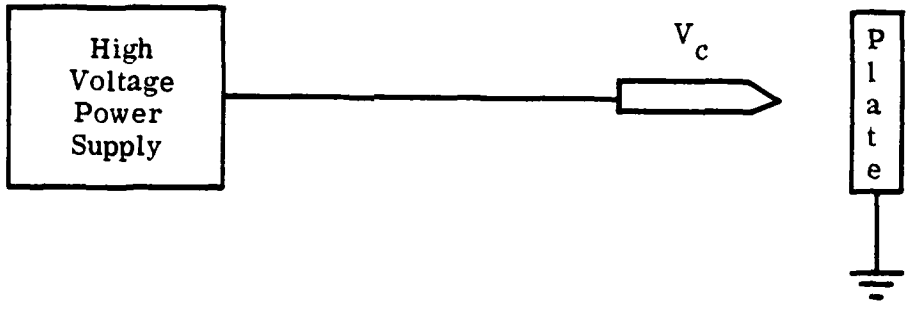

IONIZATION SOURCE

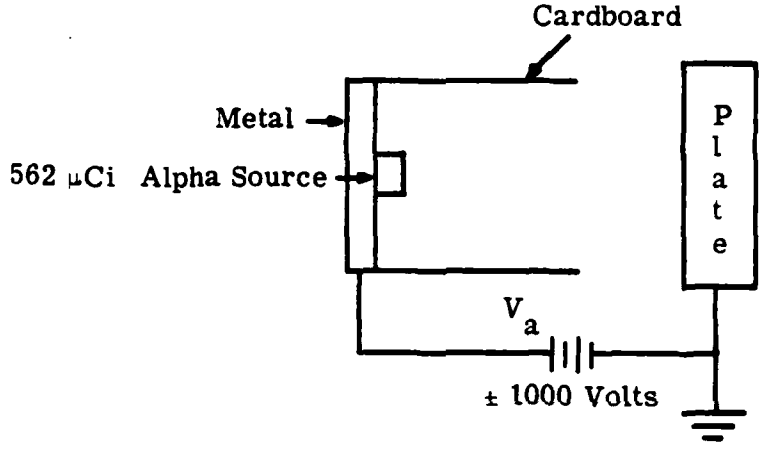

SHIELDED CORONA SOURCE

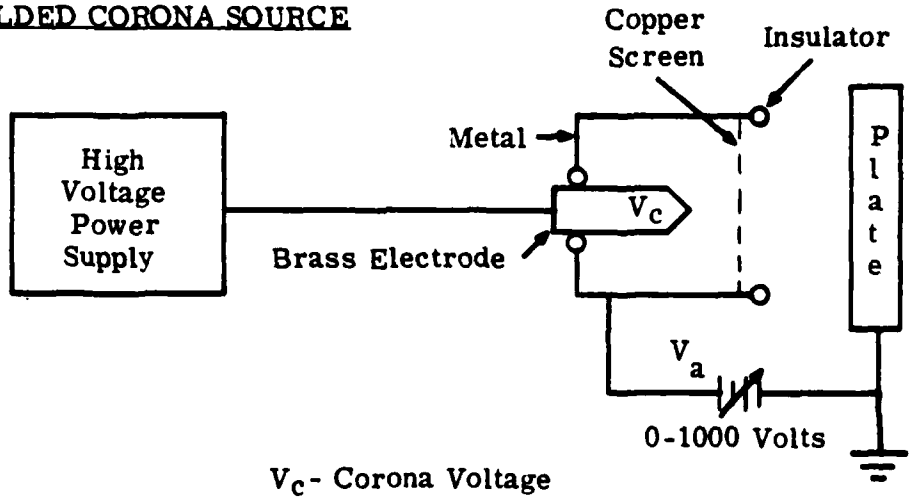

V_c - Corona Voltage

V_a - Accelerating Voltage

Figure 7 - Conceptual diagrams of three charging devices evaluated for artificial deposition of surface charge on metalic samples. The shielded corona source, which was used in our charging experiments, represents a compromise between high ion currents, provided by corona discharge, and protection of the sample plate, provided by a shielding screen.

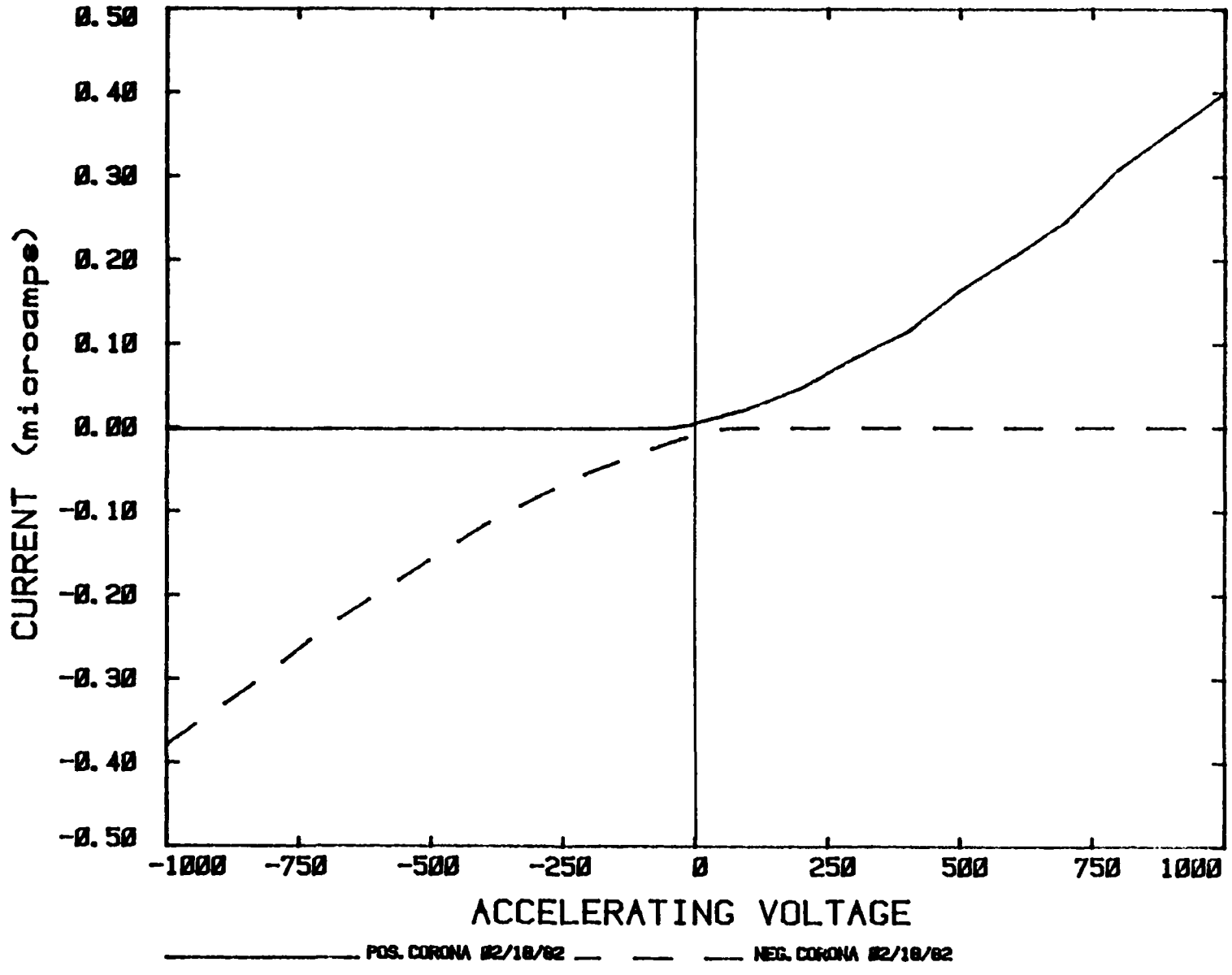

Figure 8 - Measured performance of the shielded corona-charging device. The total unipolar ion current to the sample plate is plotted as a function of the accelerating voltage applied between the screen and the plate (separated by 0.76 cm) with 6.5KV on the corona point.

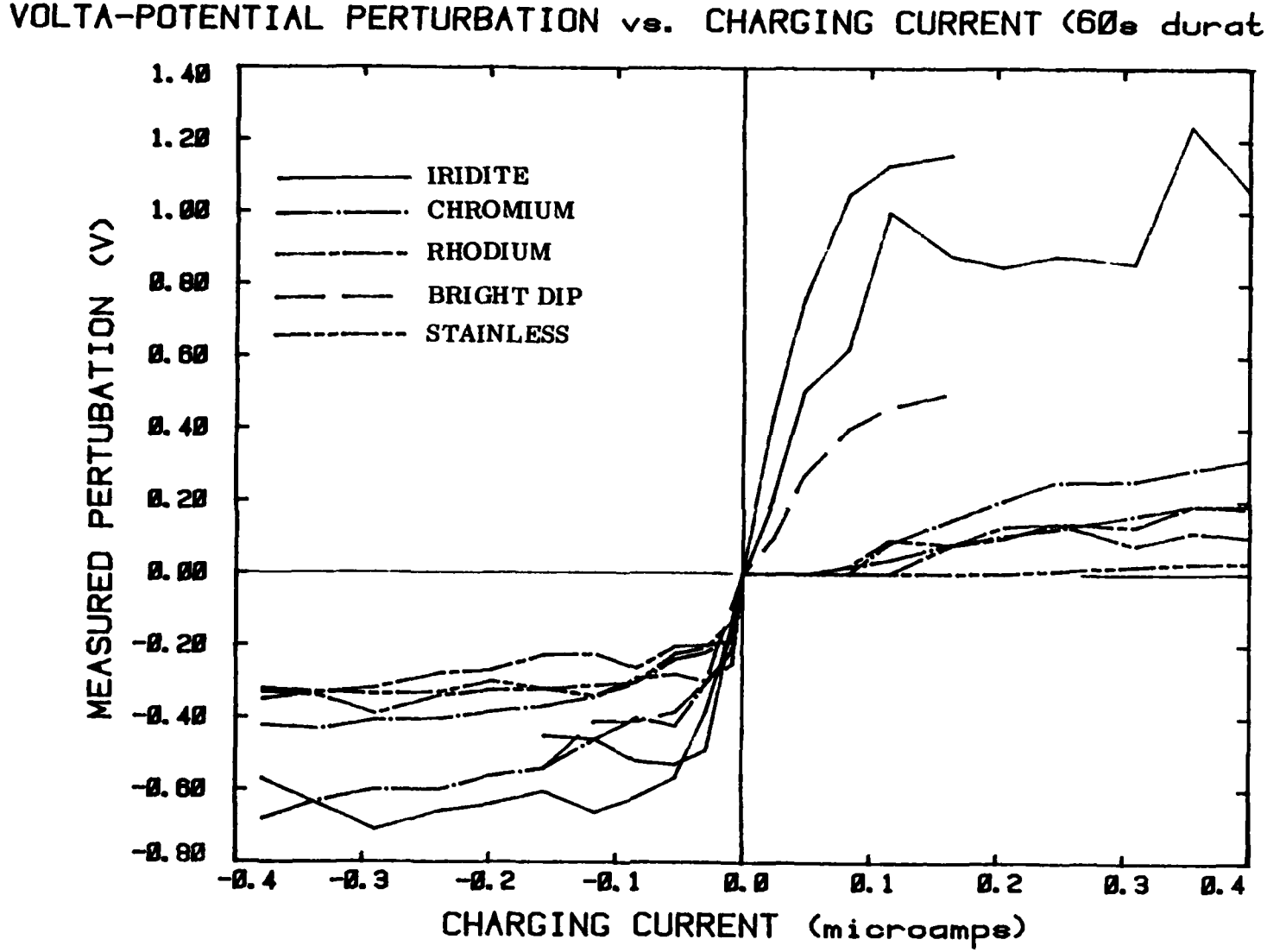

Figure 9 - Volta-potential perturbations produced on five different materials as a function of the ion current applied with the shielded corona-charging device during 60-second exposures.

Table 15. Negative Multiple Charging (Volts)

-400 V Accelerating Voltage				-1000 V Accelerating Voltage			
Rank	Surface	Mean Perturbation	σ	Rank	Surface	Mean Perturbation	σ
1.	RH2	-.272	.041				
2.	RH3	-.277	.015	1.	RH3	-.386	.038
3.	RH3	-.299	.017	2.	RH3	-.412	.022
4.	SS2	-.339	.034				
5.	RH2	-.358	.068				
6.	SS2	-.406	.078				
7.	CR3	-.442	.048	5.	CR3	-.574	.071
8.	CR3	-.478	.136	6.	CR3	-.604	.058
9.	AI3	-.575	.025	3.	AI3	-.558	.028
10.	CR2	-.606	.093				
11.	AI3	-.700	.024	4.	AI3	-.561	.026
12.	AI1	-.718	.014				
13.	CR2	-.790	.100				
14.	AB1	-.995	.043				

the dielectric and on the concentration, polarity, and depth of the trapping sites. The chargeability should also depend on the trapping characteristics and on the dielectric strength of the material. The effect of washing with water may be explicable in terms of a dipole layer of oriented water molecules on the surface, which slowly evaporates.

Chargeability Results. Figure 9 shows the Volta-potential perturbations produced on various surfaces by applying shielded corona for exactly one minute with various charging currents. Notice that the polarity and magnitude of the effect depend on the polarity and magnitude of the current, but not in a linear fashion. The figure indicates that there is considerable difference in the chargeability of the different surfaces and even of the same surface for opposite polarities. Most surfaces accept more negative than positive charging, but the reverse is true for Iridite (TM). It appears that all of the surfaces are approaching their maximum chargeability by the time the charging current reaches ±0.4 μA .

Since the maximum Volta-potential perturbations reached in our charge-deposition experiments were only about one volt, it appears that the observed chargeability is limited by the properties of the sample surface rather than by cut-off of the charging current. Therefore, we expected that surfaces could be "pumped up" to their maximum charge by increasing the charging times or by repeated exposure of the same spot, as well as by using higher charging currents. This expectation motivated the measurements tabulated in Tables 15 and 16.

These tables present the averages and standard deviations of the perturbations in apparent work function observed in a collection of multiple-charging runs with the shielded corona source operating at ±400 and ±1000V. Each run consisted of a series of ten or eleven identical, one-minute exposures of the same spot, separated by just long enough to make a measurement (about one minute). A small pumping-up effect was observed over the first two or three exposures in some of the runs, but not enough to justify segregating these data points from the averages. This pumping effect, together with the statistical fluctuctions among repeated exposures, is reflected in the tabulated standard deviations.

The rows in each table are arranged in ascending order of average

Table 16. Positive Multiple Charging (Volts)

+400 V Accelerating Voltage				+1000 V Accelerating Voltage			
Rank	Surface	Mean Perturbation	σ	Rank	Surface	Mean Perturbation	σ
1.	SS2	-.003	.014	1.	SS2	.042	.015
2.	RH2	.008	.011	3.	RH2	.061	.012
3.	SS2	-.018	.009	2.	SS2	.055	.014
4.	RH3	.024	.013	5.	RH3	.066	.031
5.	RH2	.033	.016	4.	RH2	.082	.033
				6.	RH3	.085	.020
6.	CR3	-.073	.014	7.	CR3	.201	.014
				8.	CR3	.209	.009
7.	RH2	.127	.014				
8.	CR2	.200	.035	9.	CR2	.330	.029
9.	SS2	-.206	.012				
10.	CR2	.213	.040	10.	CR2	.347	.031
11.	AB1	.800	.066				
12.	AI3	.836	.073	11.	AI3	1.15	.049
				12.	AI3	1.20	.078
13.	AI1	1.35	.020				

perturbation magnitude for the 400V runs. The 1000V runs show a somewhat different ranking, as indicated by the order numbers in the center column of each table. Notice that, in every case except that of negative charging of Iridite (TM), the charging at 1000V is substantially greater (in the polarity of the charging current) than that at 400V. Evidently pumping up by multiple charging with a 400V accelerating potential is not usually as effective as single charging with 1000V. We cannot explain this observation.

Another anomalous result apparent in Table 16 is that some materials exhibit negative perturbations due to positive charging currents. All of the multiple-charging runs with +400V accelerating voltage on stainless steel, and one out of three on chromium, had negative averages. These polarities all reversed to positive, however, in the +1000V runs. This effect did not manifest itself in the single-charging experiment leading to Figure 9, and we have no explanation for it.

The overall result of this series of experiments is that deposition of charge patches on the surface of a metal can be as important as contact between different metals in terms of creating Volta-potential differences. This makes it the most important single criterion evaluated in this report for selection of field-mill materials in situations where surface charging is likely. It is clear from the multiple-charging data of Tables 15 and 16 that stainless steel and rhodium are the best materials tested. Iridite (TM) and bright-dipped aluminum are seen to be totally unacceptable.

IV. SUMMARY AND CONCLUSIONS

The two series of experiments described herein were aimed at evaluating various metal surfaces for practical use in field mills and other atmospheric-electrical instrumentation in the natural environment. Two distinct types of measurement errors were identified to originate from the surface behavior of these metals. Variations in the work function of a metal in air can occur both from place to place on the surface and over time as a result of weathering. Similar perturbations in the apparent work function can be caused by deposition of surface charge on the natural dielectric layers which appear to exist on the surfaces of most metals.

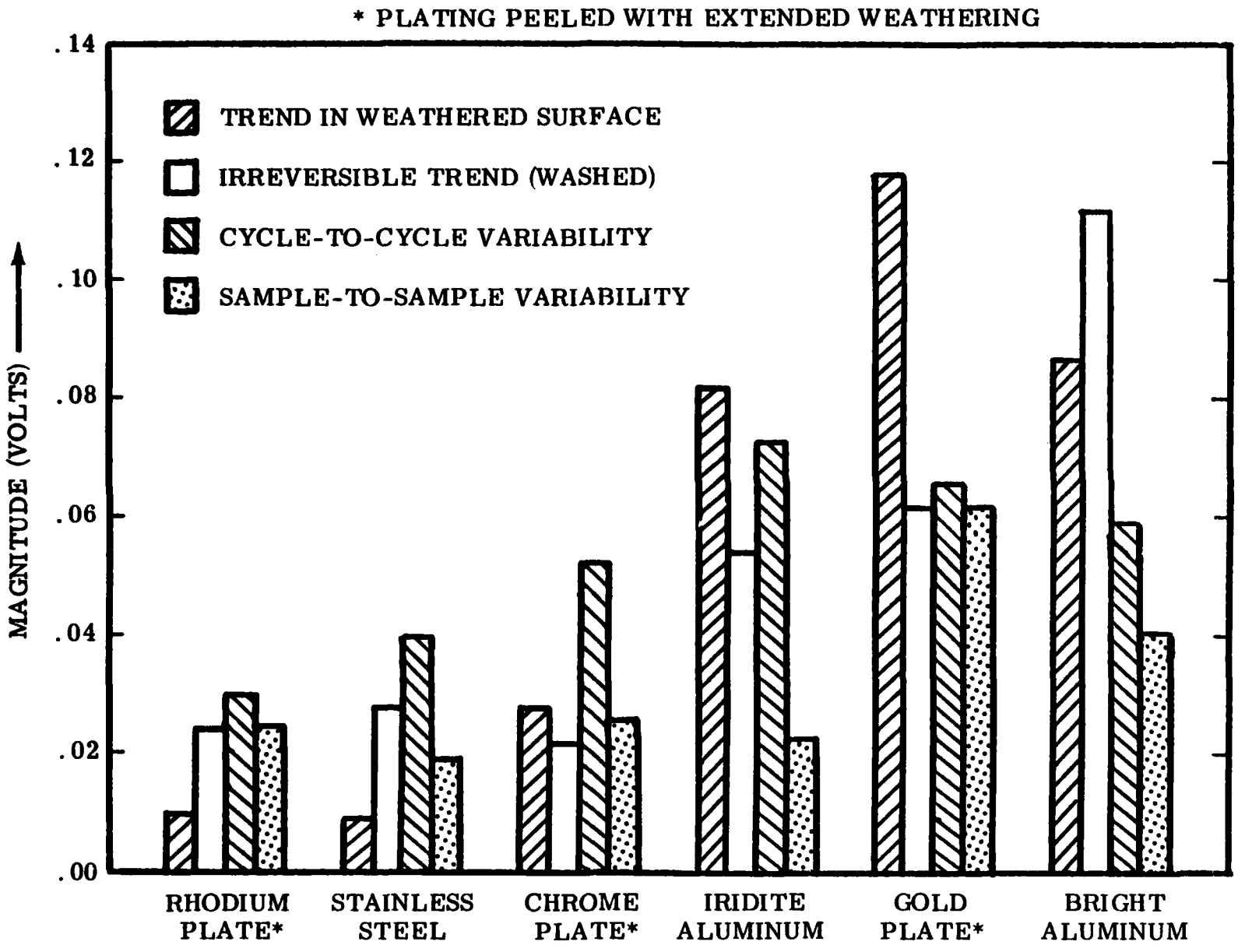

Figure 10 - Summary of weathering effects from the nulling-potentiometer experiment. The meaning of the four statistics plotted is described in detail in the text.

Since these two types of electrical phenomena are difficult to distinguish by simple measurements, separate experimental techniques were developed to explore each of them individually.

The nulling potentiometer method described in the first half of this report was used primarily to quantify the effects of weathering on contact potentials. Figure 10 summarizes the most significant results of this work. The "trend in weathered surface" is the absolute value of the slope (taken from Table 8) of a line fitted to the contact potential of the indicated material as a function of weathering repetition number, measured relative to an unweathered control. This is perhaps the most practically important measurement, since it represents a secular trend in surface properties with exposure to the elements. The "irreversible trend (washed)" is a similar absolute slope (also from Table 8) after washing a weathered plate with water and Freon (TM) to remove superficial contamination. This statistic is intended to suggest that an "irreversible" chemical change occurs on some surfaces, over and above the deposition of contaminants from the atmosphere.

The third bar in each group in Figure 10, the "cycle-to-cycle variability", is the standard deviation of the change in contact potential of a weathered plate due to washing (taken from Table 7) among all the weathering cycles. This is a measure of the repeatability of the effect of surface contamination due to weathering. Finally, the "sample-to-sample variability" is the standard deviation of the difference between the two samples of each kind (also taken from Table 7) among all weathered and washed states. This indicates the overall consistency of different pieces of the same material under environmental conditions.

The general implication of Figure 10 is that rhodium, stainless steel, and perhaps chromium are consistently and relatively slightly affected by weathering. Gold and the two forms of aluminum, on the other hand, are quite significantly affected, particularly as to secular trends in their surface properties. The largest effects observed in this series of experiments are on the order of 0.1V. In a shutter mill with a cover-to-stator spacing of one centimeter, for example, this could cause an erroneous reading on the order of 10V/m.

The capacitive probe method, described in the second half of this

report, was used mainly to explore the extent to which artificially deposited surface charge could alter the electrical properties of metals in air. Many interesting phenomena were observed (such as the differing decay times for different polarities of charging and different metals), some of which have been omitted from this report to conserve space or due to lack of consistent measurements. The primary results are summarized in Figure 11, which shows maxima and minima of the multiple-charging-run averages for each polarity of charging current, taken from Tables 15 and 16.

This figure has been drawn in a format like that of the previous one to emphasize the similarity of the results. Notice, however, that the vertical scale is compressed by a factor of more than 20. The largest perturbations here are on the order of 1.0V (as opposed to 0.1V, previously), which could cause erroneous readings on our hypothetical field mill as large as 100V/m! It appears that chargeability may be much more important than weathering sensitivity in terms of the magnitude of its effects.

We have made little effort in this report to explain our observations in terms of surface physics or electret theory. This is justified in part by the presumed complexity of our surfaces in the presence of atmospheric air and unknown contamination. The principal justification, however, flows from the purpose of our research: to obtain data for use in instrumentation design. A drastically simplified model of electret charging has been described to give the reader a physical picture of the external manifestations of charge deposition on an insulating layer. This model must not be taken as accurately describing the details of the surface structure, however. Those interested in higher levels of theoretical modeling are referred to the modern literature on surface physics.

The overall conclusion of this work is that stainless steel is an excellent practical material for the construction of atmospheric-electrical instrumentation. Rhodium plating over aluminum would be nearly as good if it could be made weather resistant. Perhaps not unexpectedly, aluminum (whether or not treated with Iridite (TM)) proved to be unacceptable. Surprisingly, gold plating over aluminum performed so badly in the weathering tests (and in its response to chamber aging -- see Table 5) that a sample was not even prepared for the lathe experiments.

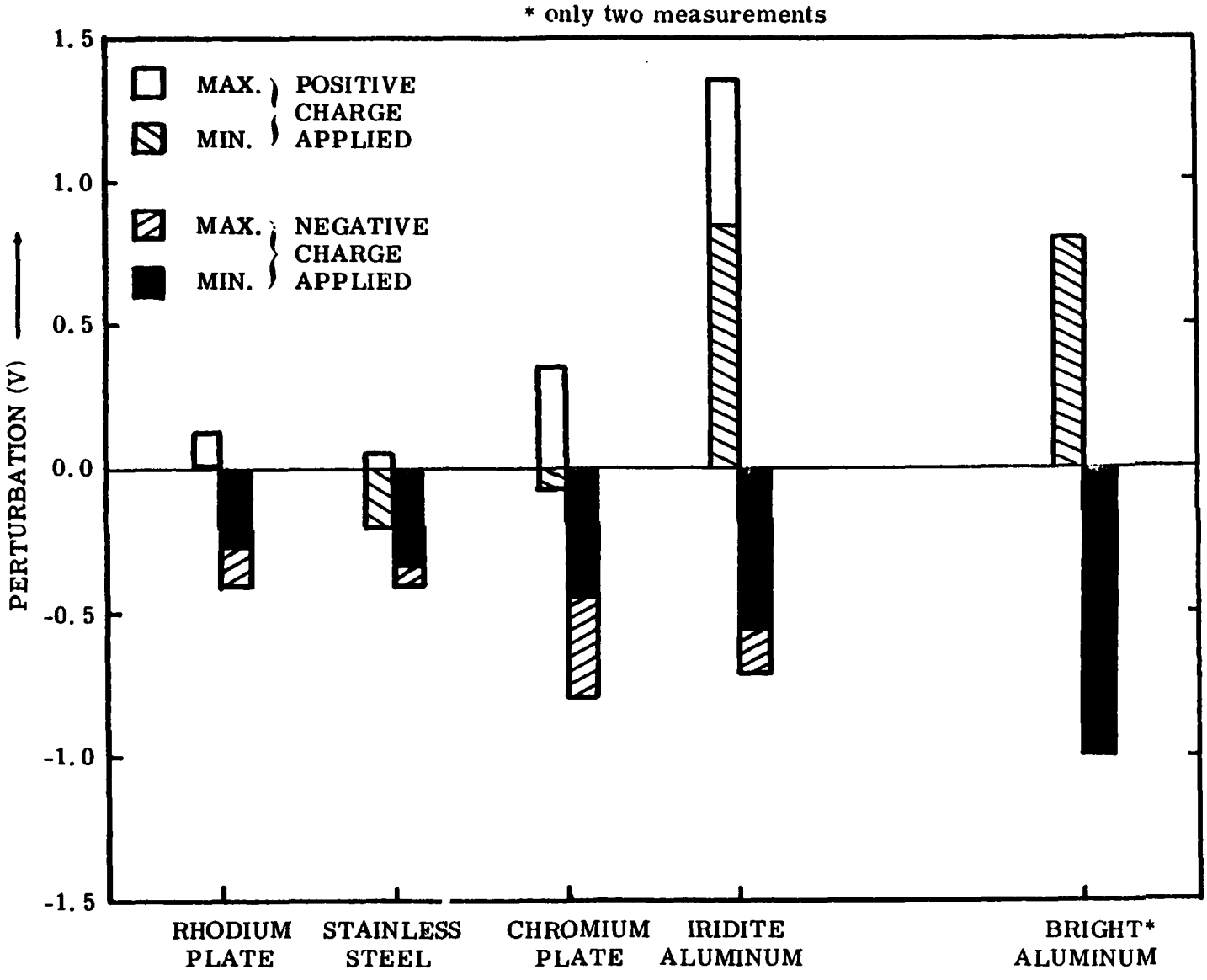

Figure 11 - Summary of chargeability effects from the capacitive-probe experiment. The maximum and minimum of the Volta-potential perturbations we observed with each polarity of applied charge are plotted for each of the metals tested. The same format has been used as in Figure 10 to facilitate comparison.

V. ACKNOWLEDGMENTS

We wish to acknowledge the many helpful discussions with and suggestions from many members of the Atmospheric Physics Branch, especially R. V. Anderson, L. H. Ruhnke, and W. A. Hoppel.

This work was supported in part by NASA's Marshall Space Flight Center on DPR H-46856B and Langley Research Center on DPR L4703B.

VI. REFERENCES

Adam, N. K. (1968). The Physics and Chemistry of Surfaces, Dover Publications Inc., New York, pp. 302-311.

Fischer, R. A. (1958). Statistical Methods for Research Workers, Oliver and Boyd, Edinburgh, p. 209.

Hoppel, W. A. (1977). "Ion-aerosol attachment coefficients and diffusional charging of aerosols," in Electrical Processes in Atmospheres, H. Dolezalek and R. Reiter, editors, Dr. Dietrich Steinkopff Verlag, Darnstadt, pp. 60-68.

Milliken, R. A. (1921). "The distinction between inrinsic and spurious contact EMF's and the question of the absorption of radiation by metals in quanta", Phys. Rev. 18:236-244.

Mohnen, V. A. (1977). "Formation, nature, and mobility of ions of atmospheric importance," in Electrical Processes in Atmospheres, H. Dolezalek and R. Reiter, editors, Dr. Dietrich Steinkopff Verlag, Darnstadt, pp. 1-16.

Sessler, G. M. (1980). "Electrets", Tropics in Applied Physics, vol. 23, Springer-Verlag, Berlin, 404 pp.

END

FILMED

6-83

DTIC